Master's Thesis

Master in Telecommunication Engineering

Design and Measurement of a Reconfigurable Antenna

Saül Horcajada Ros

Supervisor: ***Josep Parrón Granados***

Department of Telecommunication and Systems Engineering

Escola d'Enginyeria (EE)

Universitat Autònoma de Barcelona (UAB)

July 2019

El sotasignant, ***Josep Parrón Granados***, Professor de l'Escola Tècnica Superior d'Enginyeria (ETSE) de la Universitat Autònoma de Barcelona (UAB),

CERTIFICA:

Que el projecte presentat en aquesta memòria de Treball Final de Màster ha estat realitzat sota la seva direcció per l'alumne ***Saül Horcajada Ros***.

I, perquè consti a tots els efectes, signa el present certificat.

Bellaterra, *9 de Juliol de 2019*.

Signatura:

Josep Parrón Granados

Resum:

Aquest projecte es centra en l'estudi d'un concepte d'array d'antenes compacta per ser utilitzat en un sistema de modulació direccional, aquest sistema permet, a través del control de l'amplitud i la fase que alimenta cada antena, generar els símbols desitjats d'un determinat esquema de modulació en una direcció d'observació, la resta de direccions d'observació s'emet una versió distorsionada de la mateixa de manera que s'augmenta la seguretat de la transmissió.
Durant la tesi s'ha dut a terme el disseny, caracterització i validació d'un nou concepte d'antena formada per un monopol sobre una micrsostip patch antena que treballen a la frequencia d'operació de 2.45 GHz.
Finalment, després de la validació del concepte s'ha implementat una millora en forma d'un segon prototip format per dos antenes microstrip amb l'objectiu d'aconseguir una estrcutura més compacta i robusta, alhora que un grau més de llibertat per a la implementació de la modulació direccional.

Resumen:

Este proyecto se centra en el estudio de un concepto de array de antenas compacta para ser utilizado en un sistema de modulación direccional, este sistema permite, a través del control de la amplitud y la fase que alimenta cada antena, generar los símbolos deseados de un determinado esquema de modulación en una dirección de observación, el resto de direcciones de observación se emite una versión distorsionada de la misma de manera que se aumenta la seguridad de la transmisión.
Durante la tesis se ha llevado a cabo el diseño, caracterización y validación de un nuevo concepto de antena formada por un monopolo sobre una micrsostip patch antena que trabajan en la frecuencia de operación de 2.45 GHz.
Finalmente, tras la validación del concepto se ha implementado una mejora en forma de un segundo prototipo formado por dos antenas microstrip con el objetivo de conseguir una estrcutura más compacta y robusta, a la vez que un grado más de libertad para la implementación de la modulación direccional.

Summary:

This project is focused on the study of a concept of a compact antennas array to be used in a directional modulation system, this system allows, through the control of the amplitude and the phase that feeds each antenna, to generate the desired symbols of a certain modulation scheme in an observation direction, the rest of the observation directions the information is emitted distorted in order to increases the security of the transmission.
Along the thesis, the design, characterization and validation of a new concept of antenna composed by a monopole over a microstrip patch antenna that work at the operation frequency of 2.45 GHz.
Finally, after the validation of the concept, an improvement has been implemented as a second prototype formed by two microstrip antennas with the aim of achieving a more compact and robust structure, at the same time as a degree of freedom for the implementation of directional modulation.

OUTLINE

LIST OF FIGURES

LIST OF TABLES

1. INTRODUCTION

Nowadays connectivity is an overused word, the Internet of Things is becoming more deeply embedded in our day-to-day lives, soon, it will be taken for granted that pretty much any device will be able to communicate with each other creating a huge wireless network. The most significant issues of this kind of wireless data transfer is the secure transmission of confidential information.

There are many threats since this kind of traffic is easily recorded. For instance, eavesdroppers can gather information as passwords or personal data, or even modify the traffic that they use in order to transmitting spam or stealing internet bandwidth.

Because of this, a huge part of the technology evolution is focused on defence techniques in order to provide security and protect transferred data. Those technics could be implemented on various levels of the OSI (Open Systems Interconnection) model, for example, SSL protocol (Secure Socket Layer) [1] is a security technique that works from the fourth layer, called transport, to the application layer in order to encrypt and decrypt the data, this link ensures that all data passed between the web server and browsers remain private and integral. Another example is IPsec [2], is a secure network protocol that authenticates and encrypts the packets of data sent over an Internet Protocol network, third layer.

As it is shown in [3], [4], security could be also implemented in the physical layer of the OSI model. This paper presents a directional modulation technique using a phased antenna array, this option offers security due to a direction dependency, the signal will be transmitted correctly only in the line of sight to the desired receiver and is going to be distorted in the other directions. Following this concept, the present study intends to use the same principles as the previous reference and evaluate the performance of a compact antenna designed for be used for directional modulation (DM).

1.1. Objectives

According to the previous introduction, the main objective of the project is to design, fabricate and characterize a compact antenna solution that can be used to implement a directional modulation. On this purpose it is going to be built a reconfigurable antenna capable of rotating a bi-directional pattern by 360º. The antenna can reconfigure the pattern without the need for switches. It uses multiple ports integrated into a single device, with the steering realized by varying phase and amplitudes between the ports.

The antenna to be fabricated should consist of a circular patch antenna tuned on the WiFi operation frequency, 2.45 GHz, which operates at its second resonant mode, and a copper monopole, located above the circular ground plane. The switchless beamforming is achieved by means of the superposition of the radiation pattern from the two components mentioned before.

1.2. State of the Art

In this chapter is going to be introduced directional modulation of the phased array as the possibility to provide additional security level. The security problem of data transfer takes place in conventional array system when an undesired eavesdropper appears and tries to receive the transmitted information through the side lobes also generated by the array antenna.

The first researches carried out in order to solve this security problem started with time-modulated arrays which used periodic switching of elements in order to imitate a synthetic Doppler shift in order to achieve lower side lobes [5]-[7].

Afterwards differential evolution and genetic algorithms were used for pattern synthesis in time-modulated arrays [8], [9].

Then, a new techniques was proposed to synthesize a digital signal besides radiation pattern by switching array element. It was the key technique to develop to deliver a simple on-off keying [10], frequency shift keying [11], pulse-position modulation [12], or amplitude- and phase-based modulations [13], [14]. The added benefit of these thecniques is directional-dependence.

As a first approximation to our point of interest, [13] is an example of DM by means of a single driven element and multiple switched parasitic elements, which change the amplitude and the phase of the signal maintaning the constellation points that could be decoded by an intended receiver. In the undesired directions they produce different signal characteristics which scramble the constellation in order to make very difficult the demodulation. The main problem with this approach is that the sets of the parasitic elements were found by means of a trial-and-error basis, it is not a very efficient way.

Another option to implement DM is using an array with every element driven with the same CW signal, instead of the parasitics elements, the directional modulation can be implemented by changing only the element weights by means of phase shifters.

The first step of this project will be design and measure this kind of concept but using a compact structure instead of an antennas array, trying to achieve similar performance with our own design rules and, after that, is going to be develop an improvement of that concept.

Firstly, is going to be introduced an example from the papers used to inspire the project [3], [4] as a starting point.

The key component to the antenna's functionality is a circular patch milled on Taconic RF-60 substrate (εr = 6; h1 = 6 mm), which operates at its second resonant mode. It is fed using two vias of radius Rv, which form 45° with respect to the disc middle to excite two orthogonal modes.

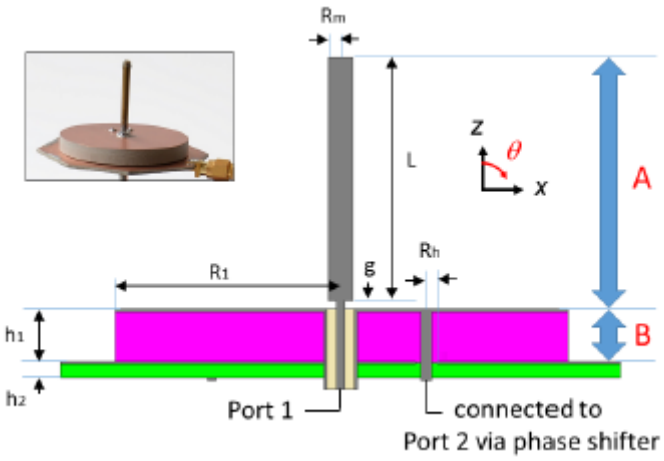

Figure 1. Antenna used for the proposed directional modulation [3]

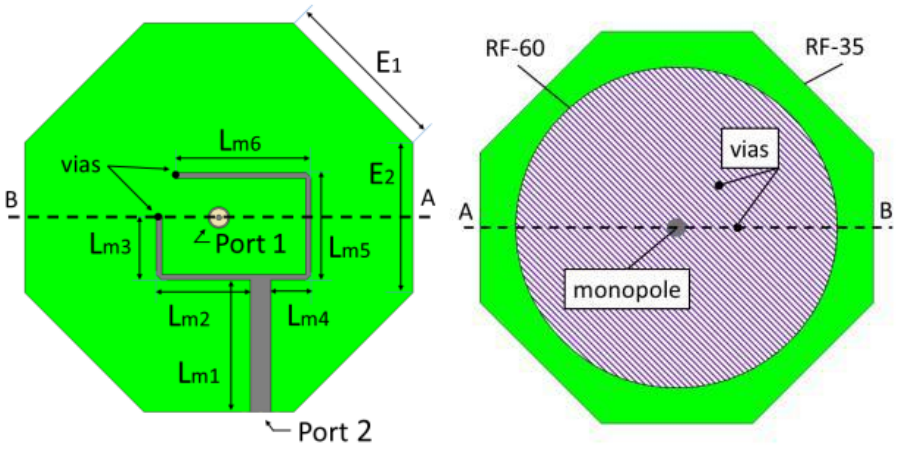

Figure 2. Bottom view and top view of the Antenna [3]

The bottom layer supports the patch feed network on the Taconic RF-35 octagonal PCB (εr = 3.5; h2 = 1.5 mm). This includes the 3 dB power divider and 90° phase shifter circuitry.

The top component is a copper monopole, located above the circular ground plane of radius R1. It is fed by a 50Ω semi-rigid coaxial cable (port 1), through the center of the lower layers. The coaxial inner conductor is connected to the monopole (of length L and radius Rm).

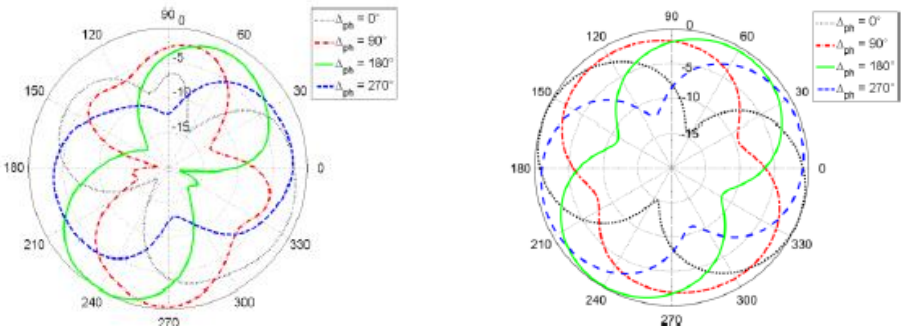

Figure 3. Measured and Simulated radiation pattern on xy-plane for various values of phase shift feedings [3]

Figure 3 shows the measured radiation pattern for four phases: 0°, 90°, 180° and 270°. It is shown, that the steering in the azimuth (xyplane) can be realized and is linearly proportional to the phase shift introduced. Some asymmetry can be seen for the phase shift of 90° configuration, especially around ϕ = 120°. This is due to the perturbation from the SMA and semi-rigid cable used to feed port 2. The right plot shows the simulated results.

1.3. Used Tools

This section describes the tools used to design, build and measure the proposed antenna.

1.3.1. Software

FEKO [15]: is a comprehensive electromagnetic simulation software tool for the electromagnetic field analysis of 3D structures. It offers multiple state-of-the-art numerical methods for the solution of Maxwell's equations, enabling its users to solve a wide range of electromagnetic problems encountered in various industries. The components that are most visible to users are CADFEKO, POSTFEKO. CADFEKO is the CAD component where the model is created and solution settings are applied. Once the model has been created, it needs to be meshed and then the kernel is run to produce simulation results. The results are then viewed, manipulated and exported in the post processor, named POSTFEKO

MathWorks MATLAB [16] is a multi-paradigm numerical computing environment and proprietary programming language developed by MathWorks. It allows matrix manipulations, plotting of functions and data, implementation of algorithms, creation of user interfaces and interfacing with programs written in other languages, including C, C++, C#, Java, Fortran and Python. It can be used for the data processing of the measurements.

1.3.2. Laboratory equipment

LPKF ProtoMat S62 [17]: an advanced circuit board plotter for in-house rapid PCB prototyping. This compact high-speed plotter provides unequalled precision and performance for quickly and easily milling and drilling circuit board prototypes in minutes. This milling machine, shown it the Figure 4 is able to operate with the maximum size of PCB equal A4 format (297x210 mm).

Figure 4. LPFK ProtoMat S62

N5242A Network analyzer [18] – the equipment made by Keysight Technologies and shown in Figure 5 is able to operate from 10 MHz up to 26.5 GHz and provide accurate S-parameters measurements.

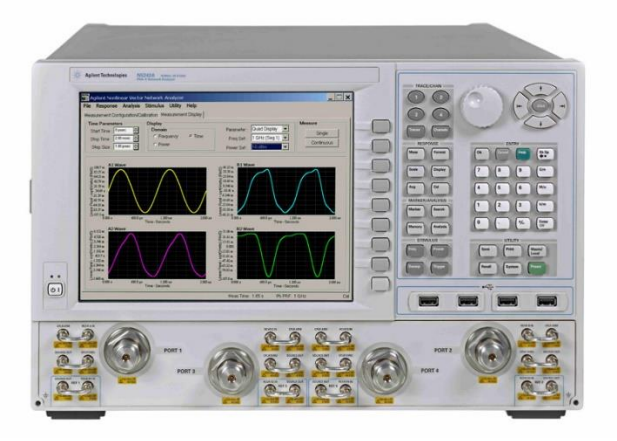

Figure 5. N5242A Network Analyzer

MVG anechoic chamber [19] Figure 6 with embedded Asysol spherical near/far field measurement system [20] is a powerful complex with RF shielding which allows performing the characterization of antennas and RF devices. It consist of a shielded chamber to avoid external interferences, which inner surfaces of the walls and floor that avoid the reflections of the RF signals that impact on the walls.

The system inside the chamber is composed by two positioners, the probe positioner and the fixation for the antenna under test. To manage those positioners there is a controller, ASYCONT, which use the software ASYSOFT that allows to rotate the probe, the positioner of the antenna under test and the antenna itself.

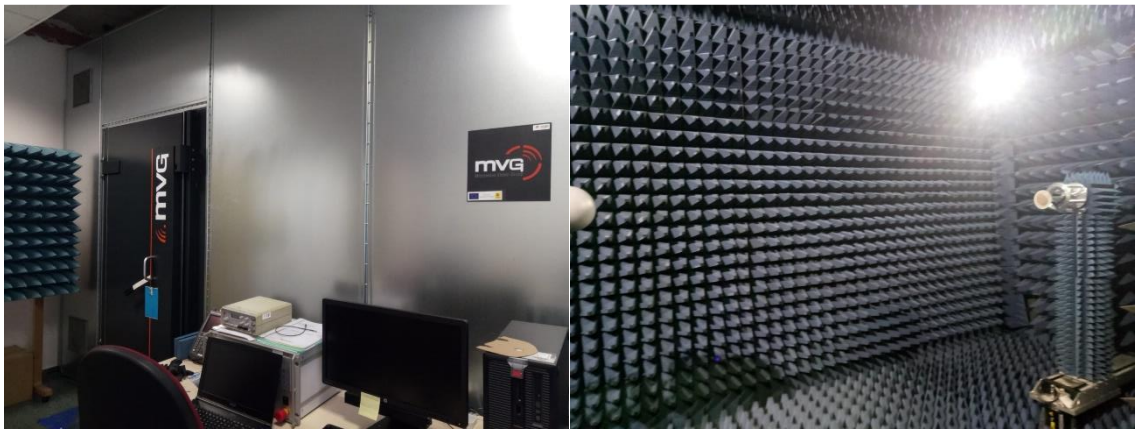

Figure 6. MVG Anechoic Chamber

1.4. Outline of the Document

This project contains five chapters. In the first chapter introduces the general information about this final master thesis, a brief introduction of the concept under investigation, the scope and the objectives are also mentioned along this section.

Chapter two is focused on the theoretical background behind the principle of directional modulation. This chapter also introduces briefly a few important concepts about the antennas under study and their main parameters.

The third chapter will be dedicated to the design and simulation, based on the theoretical basis exposed in the previous chapter. This structure will be designed by means of FEKO, starting from the evaluation of the performance of each antenna separately and finally as a unic structure.

In chapter four will the prototype will be fabricated following the guidelines and the conclusions obtained from the third chapter. Afterwards the prototype will be measured and validated by means of a comparison between simulation and measured results, focusing on S-parameters as well as the main standard radiation pattern cuts.

Finally, the last chapter describes the main conclusions explaining advantages and limitations related to this technology, and the future work derived from this master thesis.

2. FUNDAMENTAL PRINCIPLES

As presented in the introduction, this master's thesis use the principles exposed on [3], along the following chapter all this theoretical background will be explained in detail. First of all it is introduced the concept of directional modulation and, afterwards, a review of the antennas and its basic parameters is done.

2.1. Directional Modulation

The security problem of data transfer takes place when an undesired eavesdropper appears and tries to receive the transmitted information through the side lobes also generated by the antenna. Thus, the need of secure communication is greater year after year. However there are many IoT implementations constraints due to the size, cost efficient modules and low energy performance.

One of the techniques investigated in order to accomplish the constraints mentioned before is Directional Modulation (DM). This technique is able to secure wireless communications in the physical layer by means of the property of direction–dependent signal. In this way only receivers located along the specified direction will be able to capture the correct signal, while the signal radiated along other directions will be distorted. This is due to the fact that the radiation pattern produced by each element of an array of antennas is summed differently along the different directions.

In order to go deeper into this topic we are going to explain briefly a directional modulation technique using phased array, which is the one that is going to be used in this project.

Phased array is advantageous for secure transmission because it reinforces the radiation pattern in the direction of the desired receiver while suppressing the pattern in most of the other directions. However, in conventional array transmission, the same information is still transmitted in undesired directions through sidelobes, and that information can be recovered with a sufficiently sensitive receiver. In an effort to lower sidelobes and provide more secure communication, past research has explored time-modulation in arrays [21]. While conventional arrays have static element phase shifts and weighting, time-modulated arrays exploit an additional degree of freedom, time, in order to increase performance.

In order to clarify this concept Figure 7 an example of this modulation using QPSK, along the specified direction the correct constellation is formed, but in the other directions the constellations are scrambled.

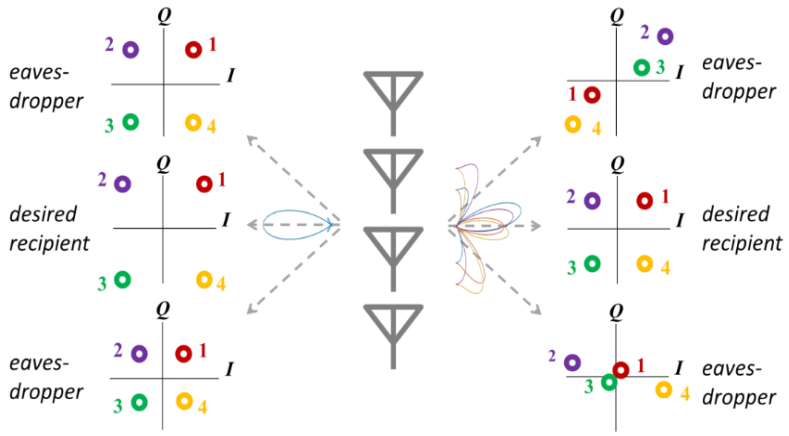

Figure 7. Conventional Modulation in Phased Arrays vs Directional Modulation in Phased Arrays [11]

Whereas in conventional modulation in phased arrays arbitrary amplitude and progressive phase shift is used to feed the elements of the array. On the other hand, directional modulation makes use of an arbitrary amplitude and phase for each element. In terms of radiation pattern, for conventional modulation the shape for transmitting symbols is the same, however, for directional modulation the shape changes at the symbol rate. Therefore, in DM, the constellation pattern depends on the observation angle as is shown in the Figure 7.

Since the constellation points in these undesired directions do not maintain their positions relative to each other, we can create constellations that are very difficult to demodulate in the presence of noise, on de contrary, in the case of conventional modulation, potential eavesdroppers can demodulate the signal if their SNR is good enough because the constellation is the same for al observation angles.

2.1.1. Directional Modulation Example

The following example (Figure 8) illustrates the difference between block diagrams of the traditional transmitter and the direction modulation transmitter. Consider a two element array with and intended receiver at broadside to the array and another undesired receiver at some direction [22].

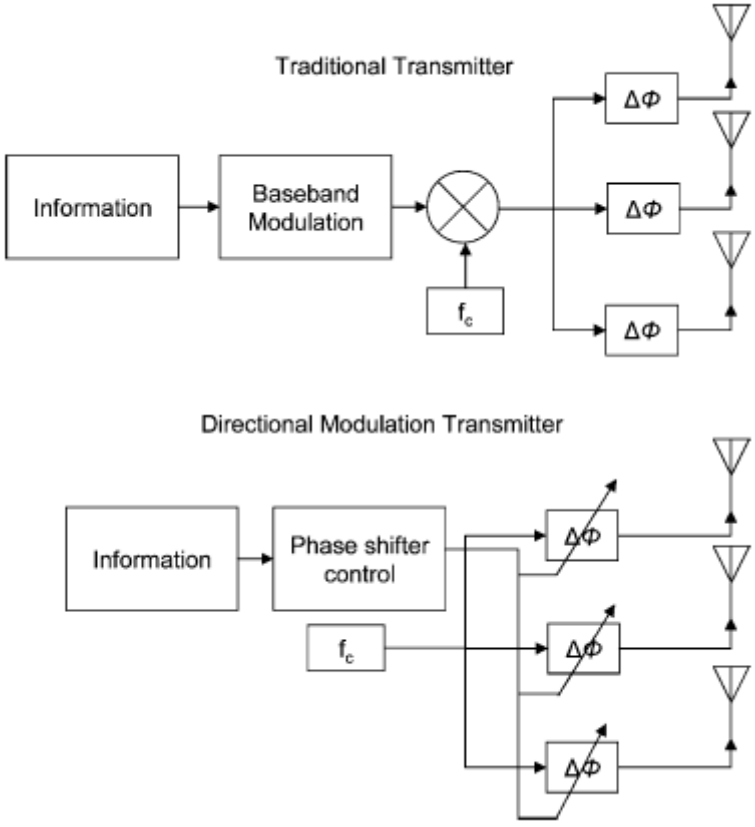

Figure 8. Traditional Array and Directional Modulation [12]

Figure 9 and Figure 10 represent an example of binary phase-shift keying (BPSK) modulation implemented with both transmitters, conventional and directional modulation. There is 30º of extra path length from the left element to the undesired receiver. The main behaviour of BPSK is multiply either +1 or -1 with the carrier frequency. In the figures are presented the voltage phasors for both recipients, desired and undesired.

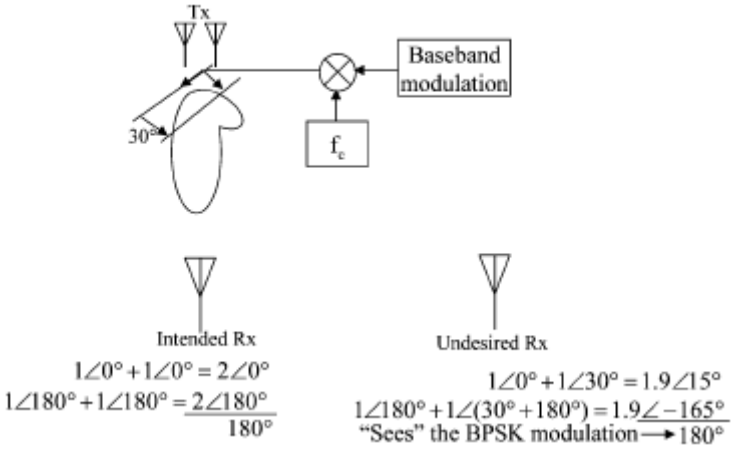

Figure 9. BPSK using traditional array transmission [12]

In the traditional array, when transmitter sends a "1" the intended receiver sees $2\angle 0°$ and $2\angle 180°$ when transmitter sends a "0". On the other hand, the undesired receiver sees $1.9\angle 15°$ when transmitter sends a "1" and $1.9\angle 165°$ when sends a "0".

The difference in amplitude at the undesired receiver is due to the extra 30 in path length from the left element relative to the right element. But these symbols still carry a 180 º phase difference between a transmitted "1" and "0". It means that if the receiver can successfully demodulate the attenuated symbols, it can receive the same information than the intended receiver received.

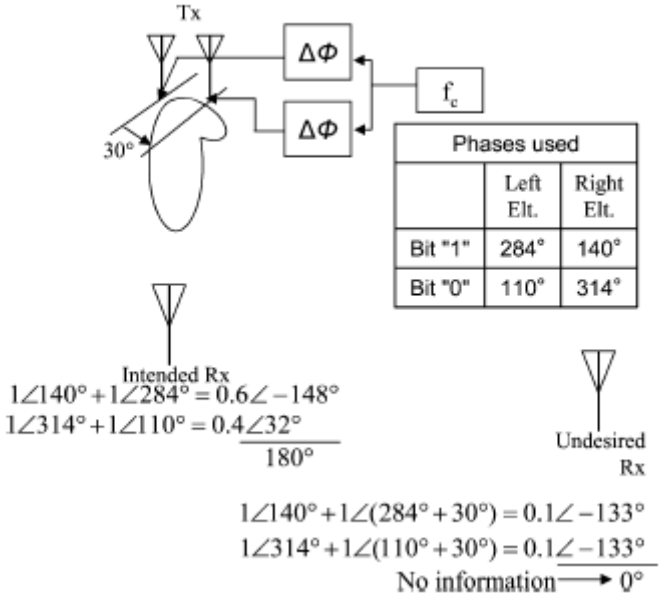

Figure 10. BPSK using DM [12]

On the contrary, in the case of directional modulation (DM) the same two-element array is used, but in this case the phases are chosen so that the intended receiver sees 180º phase difference between "1", for instance $0.6\angle -148^{o}$, and "0", for example $0.4\angle 32^{o}$, so the signal can be demodulated taking account that the signal strength is still enough.

In the case of the undesired receiver, it sees $0.1\angle -133^{o}$ when "1" is sent, and exactly the same when a "0" is sent, this means that the undesired receiver receives no information. The distortion is a consequence of the fact that the modulation is produced by the array rather than at baseband.

2.2. Antenna

The design proposed allows directional modulation without the need for a large antenna array. It consists of a compact antenna with two radiators (Figure 1): a standard quarter wavelength monopole located on a circular microstrip patch antenna that operates with two orthogonal modes TM_{21} excited with 90º phase shift, the shape of the patch antenna is due to the desire of create a circular symmetric radiation pattern from the combination of those two orthogonals modes.

While the monopole generates a radiation pattern with constant phase-shift, the circular patch creates a signal with a phase linearly dependent to the angle, this is the main property which allows replace the array of antennas by the smaller compact solution for directional modulation. The proposed technique is expected to be effective with any two antenna types, which exhibit sufficient phase variation between their radiation patterns.

The geometric phase shift between the antennas of the array is substituted by the phase shift generated by the feedings of the two antennas.

2.2.1. Micrsostrip Patch Antenna

Nowadays one of the main requirements in antennas applications is the integration constraints. Using printed circuit technology it is easy to manufacture microstrip patch antennas, which accomplish this kind of requirements without wasting excess money on it. Those structures are mechanically robust because are mounted on a rigid surface and they are very versatile in terms of resonant frequency, radiation pattern (mainly concentrated in half space) or impedance [23].

Microstrip patch antennas consist of a thin metallic strip placed above a ground plane (Figure 11). The strip and the ground plane are separated by a dielectric substrate with a certain dielectric constant, usually in the range of 2.2 to 12. The thickness of the substrate is typically much smaller than the free space wavelength. There is a trade-off between performance and integration. For better antenna performance a thick substrate with low dielectric constant should provide a better efficiency and larger bandwidth, but larger element size. On the other hand, for microwave circuitry thin substrate with higher dielectric constant presents tightly bound fields to minimize undesired coupling, but they are less efficient and with smaller bandwidths.

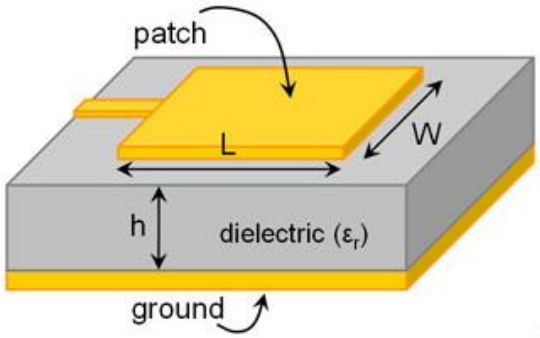

Figure 11. Microstrip Patch Antenna

The radiating patch may be square, rectangular, circular, and elliptical or any other configuration (Figure 12), the most common topology is rectangular and circular because of the simplicity of analysis and fabrication. As is said before, our shape under study will be the circular.

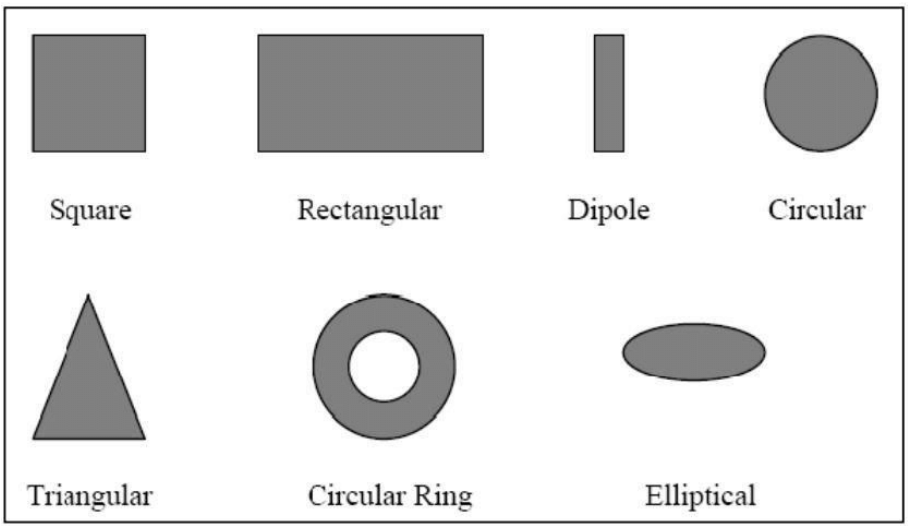

Figure 12. Microstrip Patch Shapes

The feeding those microstrip antennas can be implemented in many different ways. Some of them are microstrip line, coaxial probe, aperture coupling and proximity coupling. In the case under study the option selected will be coaxial probe by means of a SMA connector (Figure 13), where the inner conductor is attached to the radiation patch while the rest is connected to the ground plane, this is used because it is easy to fabricate and match.

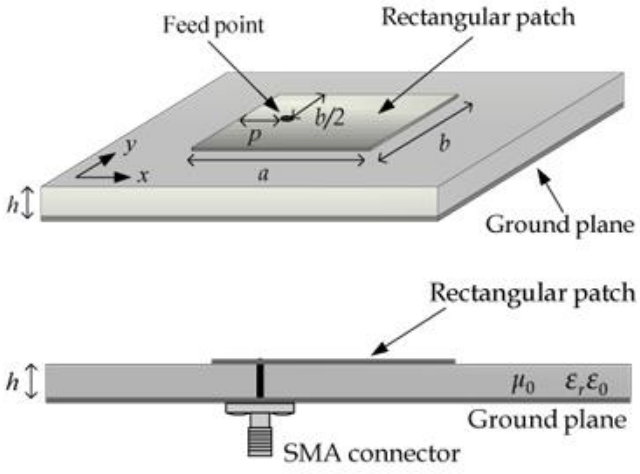

Figure 13. Feeding Point. Top and side view.

In order to analyse microstrip patch antennas behaviour the cavity model can be applied [16], treating the region between the patch and the ground plane as a cavity bounded by electric conductor, top and bottom, and magnetic walls along the perimeter of the patch, then can be found the normalized fields within the dielectric substrate.

Since thin substrates are used, the field inside the cavity is uniform along the thickness of the substrate. The cavity model assumes that the E field is purely tangential to the slots formed between ground plane and the patch edges. Moreover, it considers only TM_{nm} modes.

The fringing fields around the periphery are taken care of by extending the patch boundary outward so that the effective dimensions are larger than the physical dimensions of the patch.

The resonant frequencies of a disk antenna for the TM_{nm} mode can be found using the following approach [24]:

$$f_{nm} = \frac{X_{nm}\, c}{2\,\pi\, a_e \sqrt{\epsilon_r}} \qquad (1)$$

Where X_{nm} is the root m of the Bessel function of order n, c is the velocity of light in free space, a_e is the effective radius of the patch and ε_r the substrate permittivity.

Mode (n,m)	0,1	1,1	2,1	0,2	3,1	4,1	1,2
Root X_{nm}	0	1.84118	3.05424	3.83171	4.20119	5.317	5.331

Table 1: Roots of Bessel function

Each one of those modes has a different current distribution on the surface of the conductor disk that provides a different radiation pattern. The most usual mode is the fundamental mode that creates a maximum radiation at normal to the patch surface direction. But, in the case under study, the patch antenna will work within the mode TM_{21}, with the current distribution show in Figure 14, the contribution of two orthogonals TM_{21} modes create an omnidirectional radiation pattern in the xy-plane with a linearly dependent phase shift.

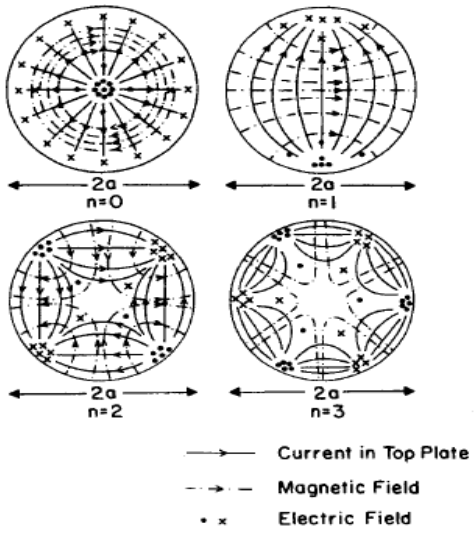

Figure 14. Fields and surface current patterns for various modes at resonance (m=1) [14].

Finally, after selecting the disk radius for a given substrate and mode the next task is to determine the feed point such that there is a good match between the input impedance of the disk and the generator impedance. Moving the feeding point along the radius the input impedance will change taking account that the maximum impedance where in the middle, where appears a null of current, and on the edges.

Within the patch two orthogonal modes of the same order, TM_{21} will be excited with a 90º phase shift, generating the omnidirectional pattern mentioned before but with the far field signal phase linearly dependent on the angle (Figure 15). This orthogonality is achieved locating the second feeding point at the same radius distance 45º shifted due to the current distribution achieving the following phase of radiation pattern in xy-plane.

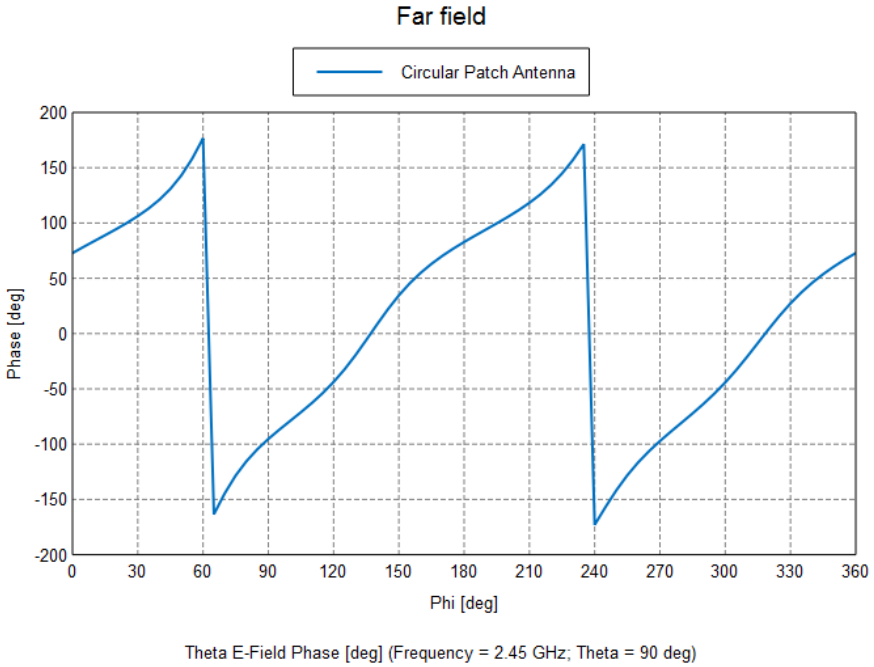

Figure 15. Phase of radiation pattern in xy-plane at 2.45 GHz.

2.2.2. Monopole Antenna

The second element of the antenna under study is a monopole antenna, this kind of antenna consists of a straight conductor mounted perpendicularly over some type of conductive surface, the ground plane (Figure 16). The feeding is attached to the lowest end of the monopole. This structure can be analysed by means of the image theory, the equivalent dipole radiates in Z>0 the same fields as the monopole [25].

Monopole antennas are half size of their dipole counterpart, with a half-wave dipole the input impedance obtained make it easy to match to 50 Ω, so with a quarter-wave monopole you can obtained also the desired radiation pattern with constant phase.

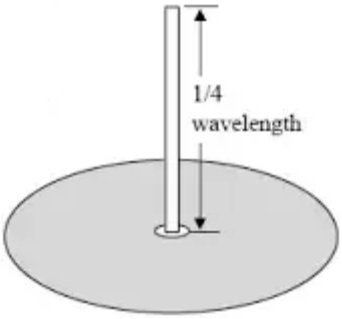

Figure 16. Monopole Antenna

2.3. Antenna Parameters

The antenna parameters are used to describes and characterize the performance of an antenna when designing and measuring them. In this subsection will be explained the most important related to this project [26].

2.3.1. Input impedance and reflection coefficient

The antenna impedance relates the voltage to the current at the input of the antenna, the impedance can be defined as Z_a:

$$\boldsymbol{Z_a = R_a + jX_a} \qquad (2)$$

Where *Ra* is the resistance and *Xa* is the reactance of the antenna, this resistance is composed by the sum of a couple of components, R_r which is the resistance of the antenna, and R_Ω which represents the loss resistance.

The reflection coefficient is the ratio used to determine the mismatch between the antenna and the source.

$$\boldsymbol{\rho = \frac{Z_a - Z_0}{Z_a + Z_0}} \qquad (3)$$

Where Z_a is the antenna impedance and Z_0 characteristic impedance of the source.

2.3.2. S-Parameters

S-Parameters or Scattering matrix describes the relationships between ports in a system, containing the reflection coefficient of each port and the transmission coefficient between them or coupling.

2.3.3. Efficiency

The antenna efficiency represents the relation between the radiated power *(W_r)* and the power delivered *(W_a)* to the antenna.

$$e_{cd} = \frac{W_r}{W_a} = \frac{R_r}{R_r + R_\Omega} \qquad (4)$$

2.3.4. Bandwidth

The bandwidth is the range of frequencies within which the performance of the antenna conforms a specified standard, where parameters as reflection coefficient is better than a certain value previously stipulated.

2.3.5. Radiation pattern

The radiation pattern of antenna is a representation of the distribution of the power radiated from the antenna (in the case of transmitting) or inflowing (in the case of receiving antenna) as a function of direction angles from the antenna.

It is defined for large distance from the antenna (far field), where the spatial distribution of the radiated power does not depend on the distance from the radiation source is independent on the power flow direction.

Usually, for radiation pattern representations are used the standard spherical coordinates, where θ is the angle measured off the z-axis, and ϕ the angle measured counter clockwise off the x-axis.

2.4. Conclusions

Finally, from this study can be extracted some conclusions:

1. Directional Modulation is a technique for security in physical layer for wireless communications.
2. A large array of antennas can be replaced by a compact solution by means of a phase shift between the port feedings. This compact solution is composed by a monopole above a patch antenna with two orthogonal feeding points.
3. The patch antenna works in the mode TM_{21} instead of the typical fundamental mode.

4. The operating frequency of the patch antenna can be controlled by means of the patch radius, the smaller antenna the higher frequency.
5. Two orthogonal feedings of the patch with a phase difference of 90º create a radiation pattern with a linear variation of the phase with ϕ in the XY plane and the monopole creates a constant phase over the XY plane.

3. ANTENNA DESIGN

As it has been discussed until now, the proposed radiating system is mainly composed by a monopole located on a circular microstrip patch antenna that operates with two orthogonal modes TM_{21} exited with 90º phase shift, the two feeding points of the patch antenna have to be shifted between them geometrically 45º.

This chapter will be focused on the design of this two elements and their integration as a compact reconfigurable antenna for 2.45 GHz. The radiation pattern analysis will be by means of the theta component because in the monopole the phi component is almost null and these criteria will be kept along all the project.

3.1. Specifications

As a first step of the design process it is needed to define the requirements of the antenna system. The requirements can be seen in the following table. The prototype will be fabricated over TRF-45 substrate because it is the one that is available in the antenna laboratory.

Requirement		Value
Operation frequency		2.45 GHz
Antenna matching		$S_{11} = S_{22} \leq -10$ dB
Coupling		$S_{21} \leq -10$ dB
Dielectric substrate	Material	TRF-45
	Permittivity	$\varepsilon_r = 4.5$
	Thickness	h = 3 mm
	Loss tangent	Tanδ = 0.0035

Table 2. Antenna Requirements

3.2. First Prototype

Firstly each part of the antenna structure is going to be designed separately, starting with the circular patch antenna.

3.2.1. Patch Antenna

Based on the discussions carried out in the second chapter, in order to achieve the desired performance the mode TM_{21} was chosen, and it was designed for the operation frequency of 2.45GHz. It will be excited by means of a coaxial probe.

In order to find the right dimensions of the patch antenna for the chosen substrate, the equation (1), explained in the last chapter, will be implemented in cadfeko, where the root X_{nm} is 3.05424.

As a first approximation in the simulation, the patch antenna will be designed and simulated for an infinite ground plane, taking account that the dimensions that can be tuned are the patch radius and the location of the feeding points, because the dimensions related to the substrate are constrained by the requirements due to the material that we have in the laboratory.

For the antenna tuning, and looking at the expression (1) shown before, it can be concluded that reducing the patch radius the operation frequency will be higher. And in terms of feeding point, if the point is moved to the edge of the antenna or to the middle, where the currents are zero, the absolute value of the input impedance will rise.

3.2.1.1. Patch Antenna infinite ground plane

The structure of the circular patch antenna with a radius of 28.1 mm shown in Figure 17, made of perfect electric conductor (PEC), and with the feedings points positioned on a radius of 14 mm from the middle, was obtained for an infinite ground plane.

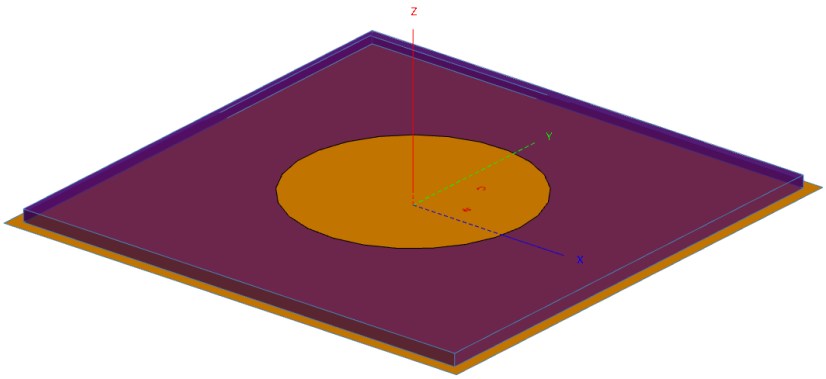

Figure 17. Circular Patch Antenna infinite ground plane

The magnitude of currents and the radiation pattern of the designed circular patch can be found in Figure 18. It can be seen that the obtained results for the current distribution is exactly the expected for the TM_{21} mode, with the four maximum and the current null in the middle. The theta component of the radiation pattern is also the expected one, with the four lobes, in order to obtain the omnidirectional radiation pattern with the combination of both orthogonal modes.

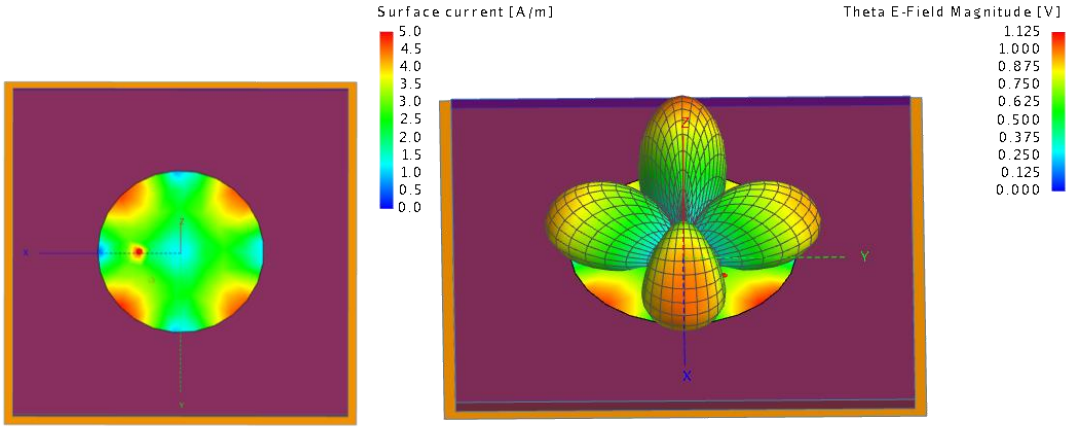

Figure 18. Circular Patch Antenna infinite ground plane Currents and Radiation Pattern Theta component at 2.45GHz

In terms of reflection coefficient, as it can be seen in Figure 19, the antenna has a good matching at the desired frequency, but as it was expected, quite narrow bandwidth. Each one of the frequencies where the reflection coefficient is below -10 dB in the figure corresponds to the different operation modes of the patch antenna, each one with a different surface current distribution and different radiation pattern.

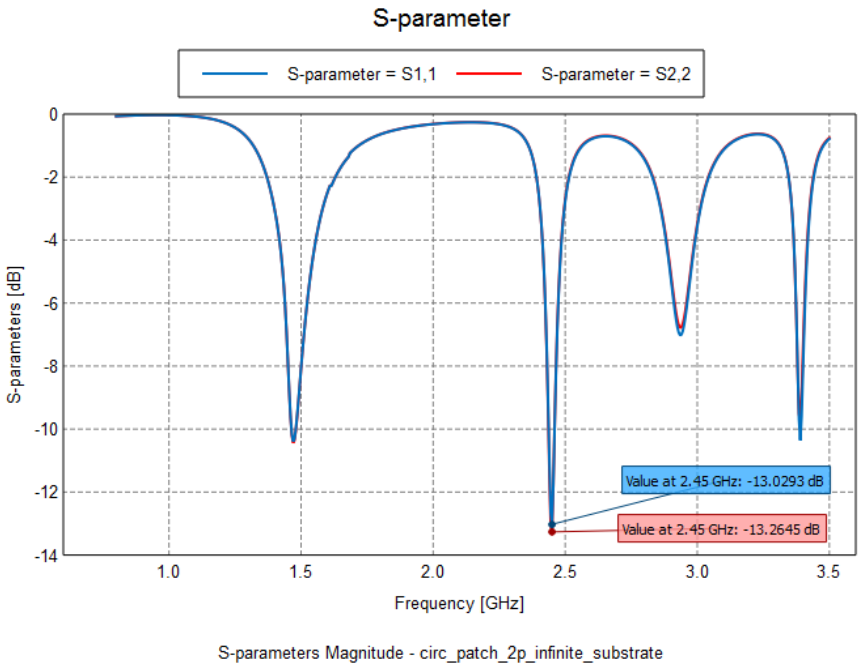

Figure 19. Circular Patch Antenna on infinite ground plane S-Parameters

3.2.1.2. Patch Antenna finite ground plane

After the desired results with infinite ground plane the following step was to simulate the structure using a finite ground plane. In the first simulation it was found that the matching was significantly shifted, now the dimensions of the ground plane is a new designing variable and there are some radiation that goes to backwards. And also, the fringing fields in the edge of the patch, as it is explained in the previous chapter the result of this effect is that the effective dimensions are larger than the physical dimensions of the patch and, because of that, the operation frequency is lower than the expected.

Once the corrective tuning is done, and the operation frequency is 2.45 GHz again, the dimensions are 27.2 mm for the patch radius and 38.1 mm for the substrate radius, the feeding points are located to 16.3 mm from the middle.

There are some differences are seen between both radiation patterns, there appears the four lobes but with the finite ground plane, as is said before, some energy is radiated to bottom (Figure 20). In the case of the infinite ground plane all the energy is radiated to the top part of the surface.

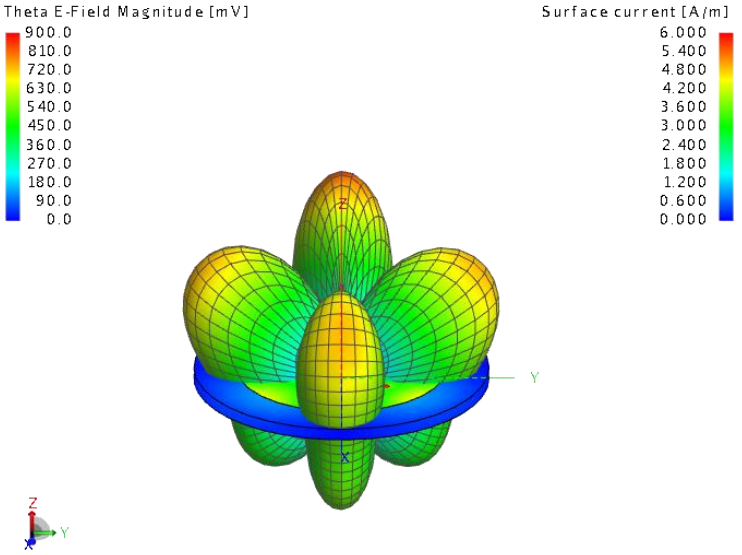

Figure 20. Circular Patch Antenna finite ground plane Radiation Pattern Theta component at 2.45GHz.

In terms of S-parameters (Figure 21) both matching are good, less than -10 dB, and the isolation between the two feeding points is still good, below -20 dB this means that the mutual coupling effect is small due to both feeding points are orthogonal between them.

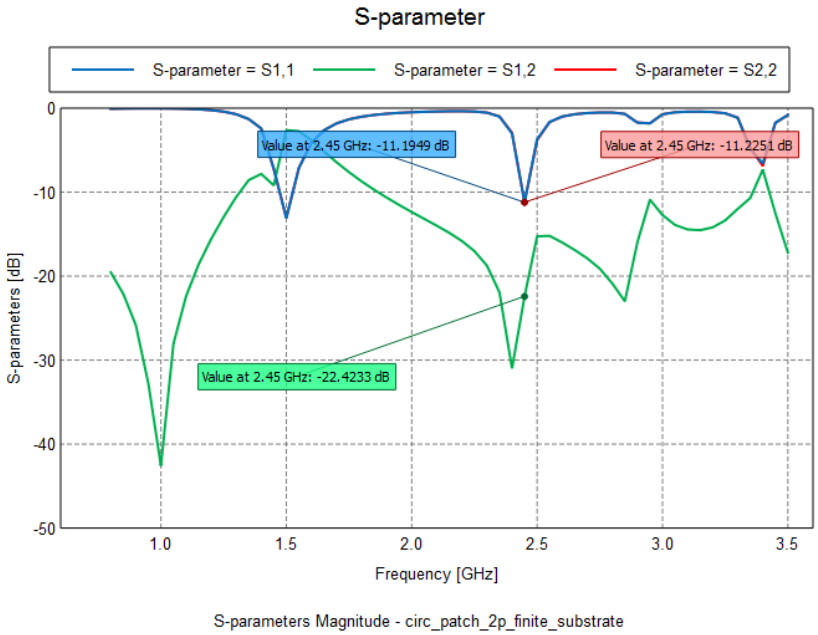

Figure 21. Circular Patch Antenna finite ground plane S-parameters

3.2.2. Monopole Antenna

As it was mentioned above, the second element of the structure is a monopole antenna above the patch. In order to design this element separately is going to take account the dimension of the patch designed before as a ground plane below the monopole.

Due to the monopole behaviour is similar to the half size of their dipole counterpart, and we are looking for an omnidirectional radiation pattern and an easy monopole to match to 50Ω, the dimensions chosen is the half-wave dipole, but in terms of monopole, a quarter-wave. Figure 22 shows the monopole of 2.92 cm over a ground plane of 40 mm of radius.

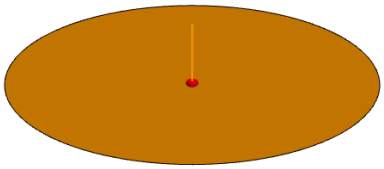

Figure 22. Monopole

In terms of reflection coefficient the value at 2.45 GHz is below the desired -10 dB, and it can be seen that the amount of frequencies below this value more wideband than in the case of the patch antenna.

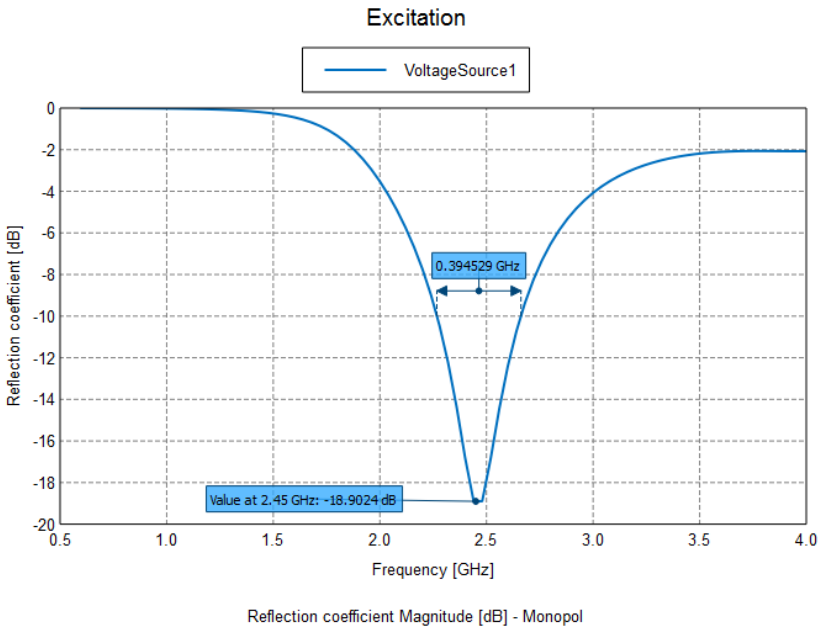

Figure 23. Monopole Reflection Coefficient

The radiation pattern is also the expected one, omnidirectional, slightly pushed up due to the effect of the finite ground plane.

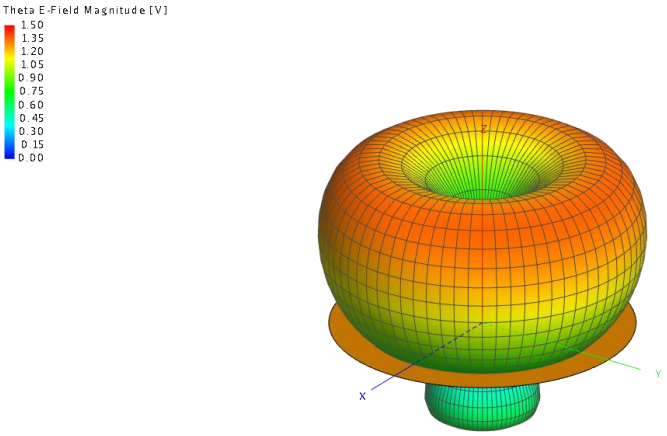

Figure 24. Monopole Radiation Pattern at 2.45 GHz

3.2.3. First Prototype Simulation Results

Finally, both elements are built together getting the structure shown in the following figure. The monopole over the circular patch, with a total of three ports. Taking account that this was the last simulation before the prototyping it was much more accurate than the approximations made before.

Figure 25 shows the structure where the patch radius is 27 mm, the substrate radius is 37.8 mm and the monopole length has a value of 3.09 cm. The patch feeding points are located in a radius of 13.23 mm, with a difference between them of 45º as is said before.

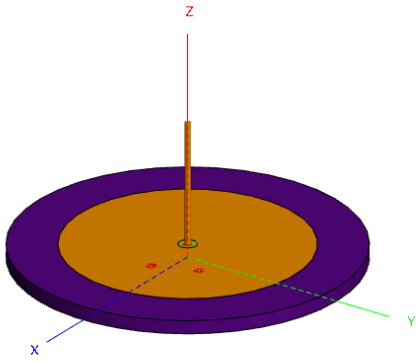

Figure 25. Proto1

The matching for the three ports are good, port 1 and 2 are the patch feeding points and the port 3 is connected to the monopole, it can be found in Figure 26, both patch ports are -10 dB and the monopole below -8 dB. In terms of isolation all of them are under -25 dB. Everything suggests that the prototype will have the desired performance.

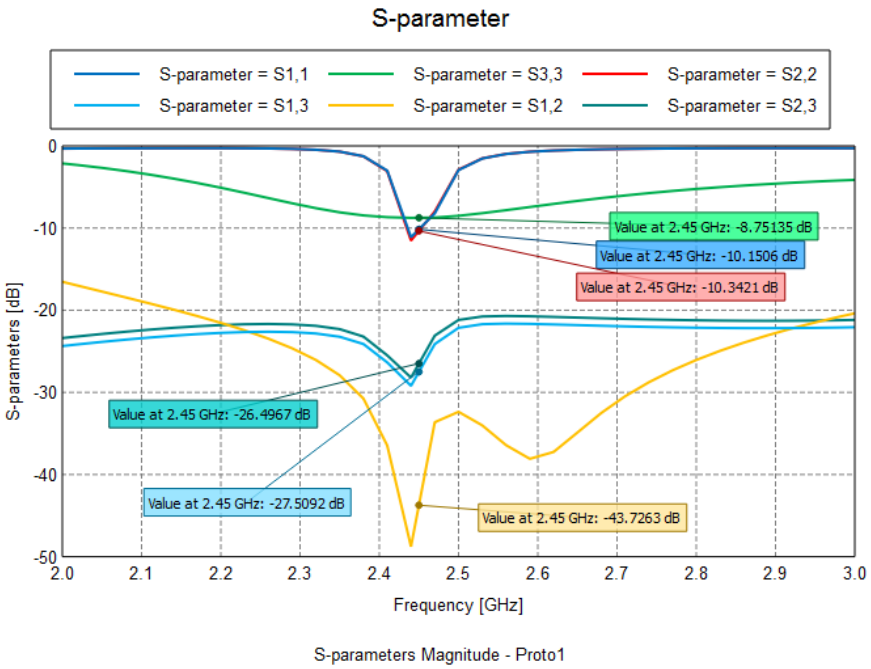

Figure 26. Proto1 S-parameters

The efficiency (Figure 27) of each ports is simulated separately with a 50Ω charge in the others ports, will be 70% for the patch and around 45% for the monopole probably due to the coupling effects between patch ports was better than between patch and monopole and some of the radiated energy from the monopole goes to both patch ports.

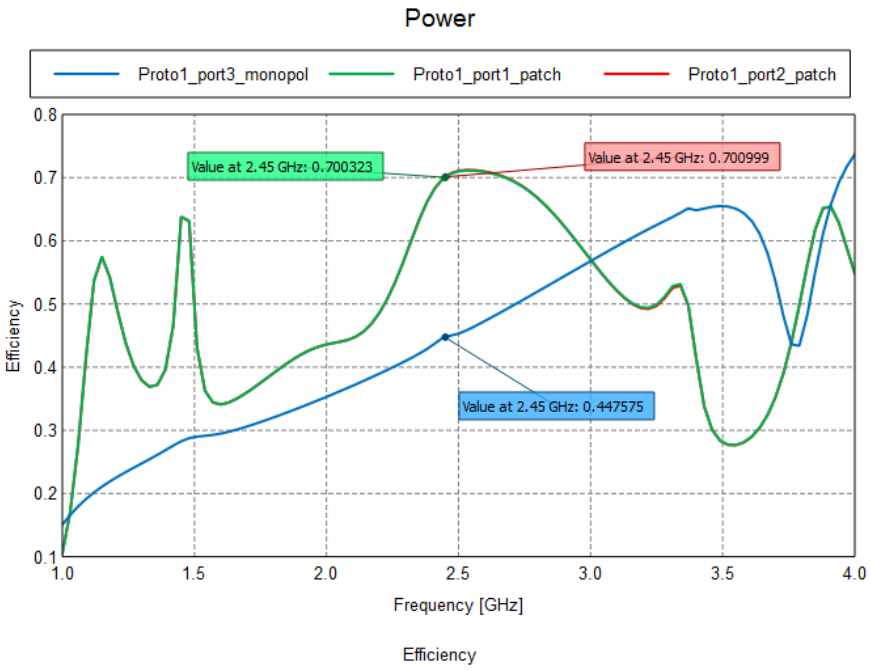

Figure 27. Proto1 Efficiency

Looking at the far field phase of each element separately (Figure 28 and Figure 29), with a 50Ω charge in the others ports, it can be seen are obtained the desired performance, in terms of magnitude it can be seen that the combination of both patch ports results in to an almost constant value and the monopole magnitude is almost constant itself.

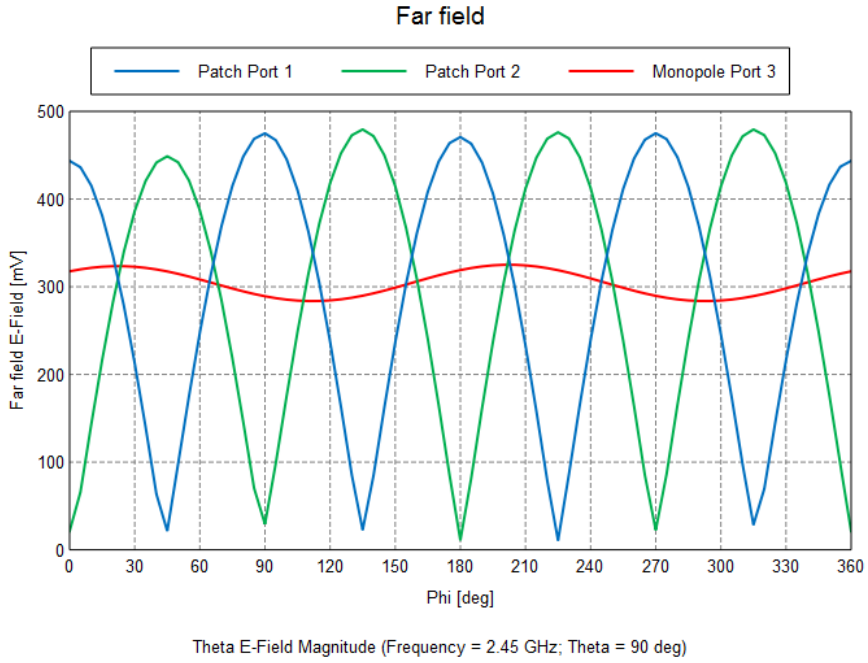

Figure 28. Proto1 Far Field Theta component Magnitude at 2.45GHz

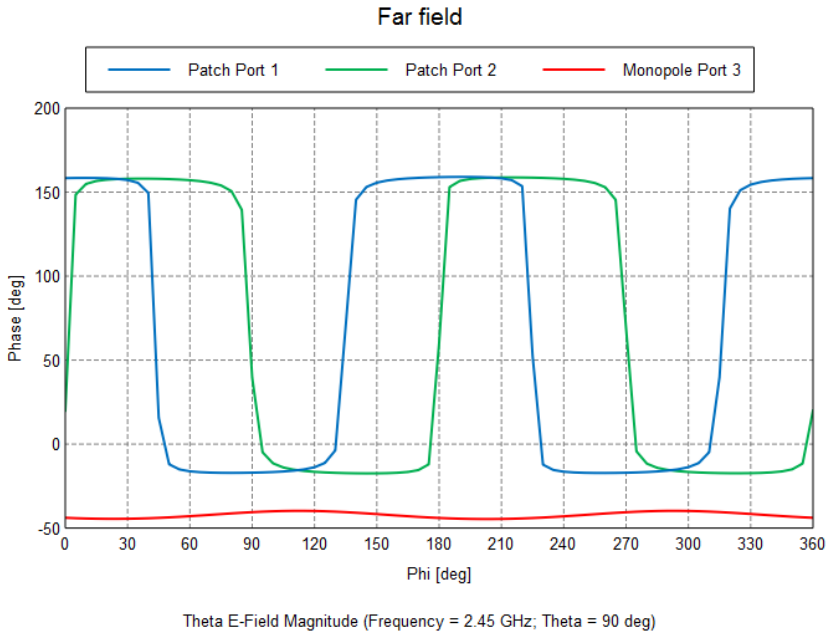

Figure 29. Proto1 Far Field Theta component Phase at 2.45GHz

After the combination of both feeding points of the patch fed with a 90º shift phase, simulating the feeding in both patch ports and the monopole charged with 50Ω, is created the expected angle dependence and, in the case of the monopole, the almost constant phase.

Figure 30 shows the periodicity of the points where both phase are matched, this periodicity is the culprit for the bidirectional in the functionality.

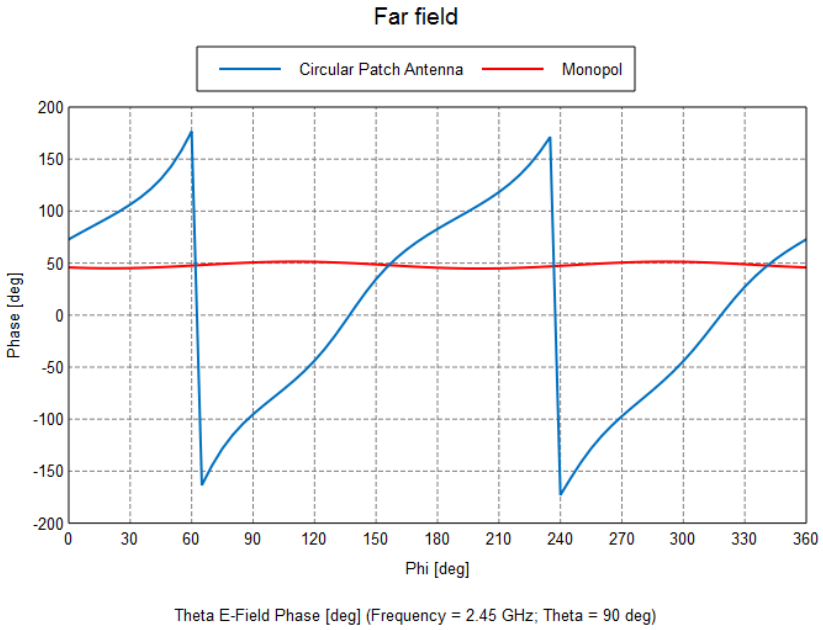

Figure 30. Proto1 Far Field Theta component Phases combined

As a last step in the simulation is going to take a look to the real functionality of the compacted antenna, feeding the two ports of the patch with a phase shifted 90º as was explained in the second chapter, and, changing the phase of the monopole will be achieved the rotation of the radiation pattern.

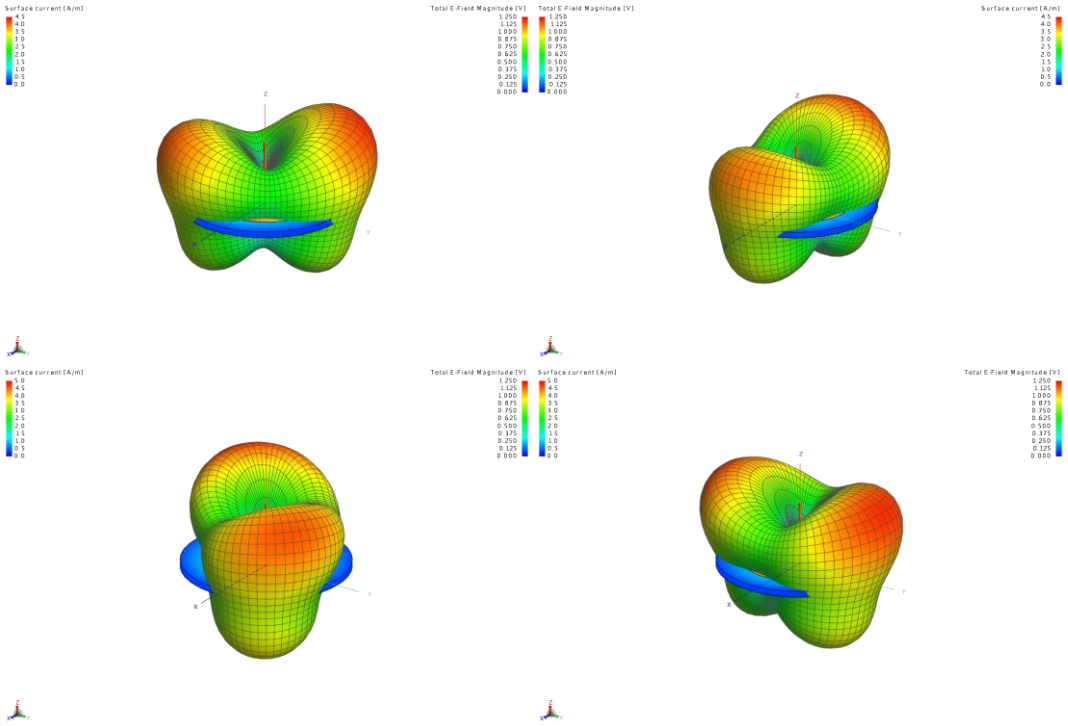

Figure 31. Proto 1 Radiation Pattern: a) 0º phase shift; b) 90º phase shift; c) 180º phase shift; d) 270º phase shift.

Figure 31 shows the expected behaviour of the system, the phase difference between patch and monopole here 0º, 90º, 180º and 270º. There are two opposite maximum lobes which are rotating through the phase shift.

Figure 32 illustrates the cuts at theta 90º superposed validating the desired performance exposed during the second chapter.

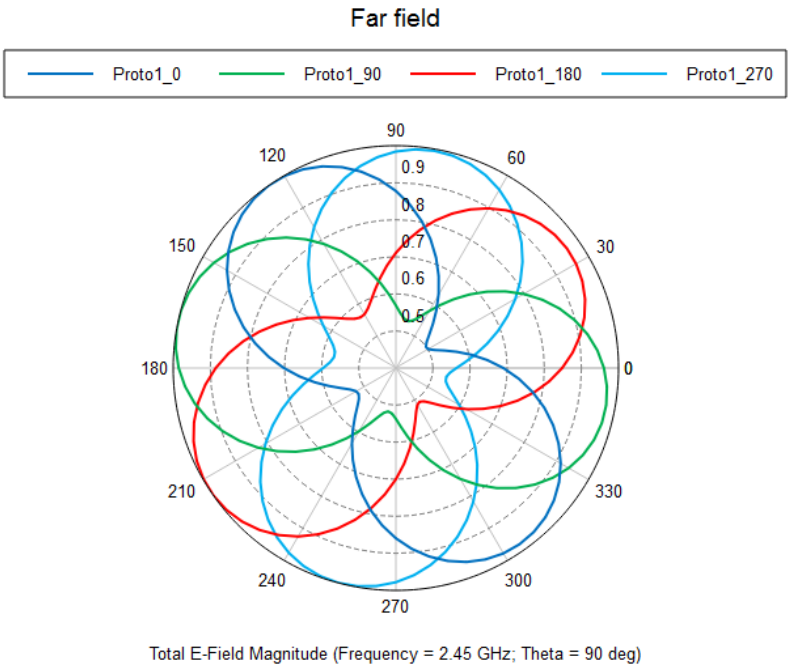

Figure 32. Proto 1 Polar Radiation Pattern Theta 90º at 2.45GHz

3.3. Second Prototype

After this first prototype, done following the idea from the references exposed along the state of the art, as a next step for the project, a new prototype will be built trying to improve the performance of the radiation pattern. As it can be seen in the first part, the radiation pattern has two opposite maximum lobes due to the periodicity in the combination of the circular patch and the monopole.

This performance can be improved adding degrees of freedom in the combination of the radiation pattern, instead of 3 ports, the following step will be create a new concept with 4 ports

This second prototype is composed by a patch antenna working on TM_{21} over a bigger patch antenna working on TM_{31}. Moreover, the second prototype is going to be more compact and more robust due to the elimination of the monopole.

In order to show the behaviour in an easy way in that study, the feeding phase between the two ports of the same circular patch will be fixed to 90º or -90º in order to create two times the same linear dependence to the angle in the phase for the far field as the shown in the other prototype (Figure 30).

The key in the design of the feeding is find exactly the feeding point where two orthogonal modes are excited on the same patch, as in the case shown before, but using points where the mutual coupling between both patches is lowest, keeping the geometric symmetry along the design.

3.3.1. Patch Antenna

Those two elements will be designed following the rules for microstrip patch antennas shown in the first prototype. Using the same substrate and implementing the equation (1). Where the root X_{nm} is 3.05424 for the patchTM_{21} and 4.20119 for the TM_{31} [24].

3.3.1.1. Patch Antenna TM_{21}

In the case of the patch antenna TM_{21}, the design is more or less the same than in the first prototype, using the same dimensions as in the other case, the two feeding points for the orthogonal modes at 45º, achieving the same behaviour than before. But after the integration with the other patch the design must be tuned in order to maintain the performance.

3.3.1.2. Patch Antenna TM_{31}

This second patch antenna will be bigger due to the root necessary for the mode TM_{31}. The currents and the radiation pattern of the designed circular patch can be found in the figure 24. It can be seen that the obtained results for the current distribution is exactly the expected for the TM_{31} mode, with the six symmetrical maximums and the current null in the middle (Figure 33).

In order to excite two orthogonal modes TM_{31}, the feeding must be geometrically shifted a multiple of 30º.

The structure is composed by the patch of radius 37.9 mm, with both feeding points with a radius of 19 mm from the middle and with a substrate of 53 mm.

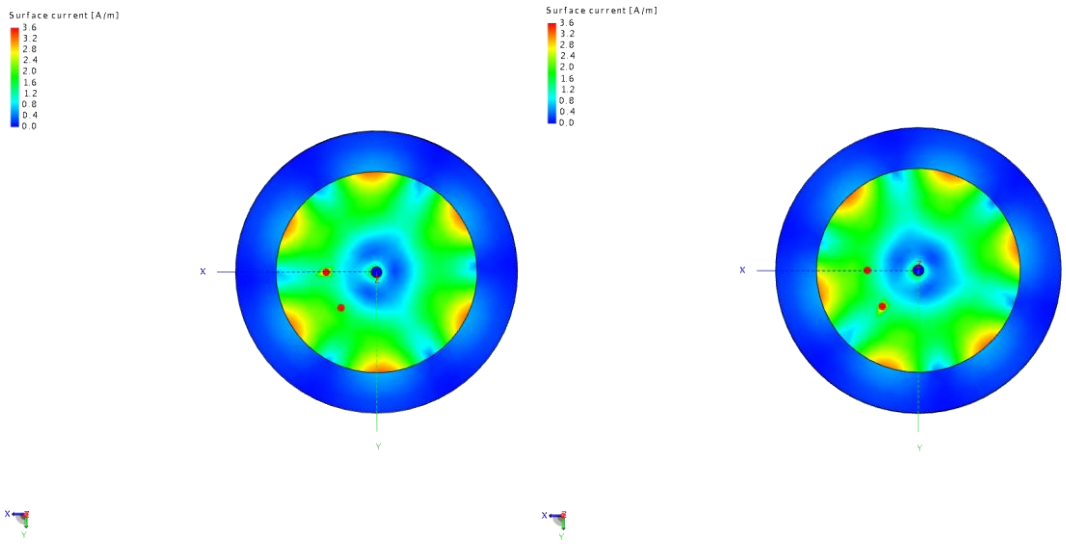

Figure 33. Patch Antenna TM_{31} Currents for both orthogonal modes at 2.45GHz

In terms of radiation pattern is more or less the expected one, the pattern through the XY plane has six lobes instead of the four shown in the TM_{21}, with the null on Z axis (Figure 34).

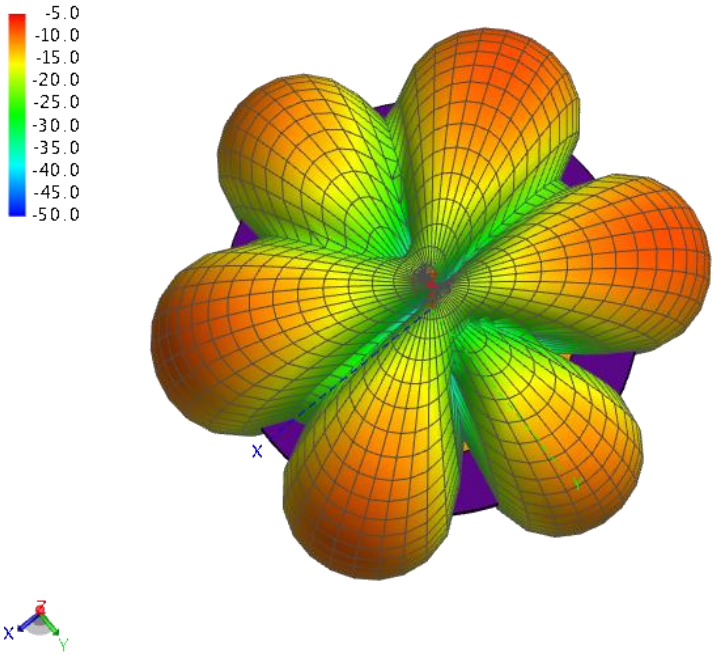

Figure 34. Patch Antenna TM_{31} Radiation Pattern Theta component at 2.45GHZ

3.3.2. Second Prototype Simulation Results

Finally, after the properly study of each element, the whole prototype is built. It can be seen the TM_{31} circular patch, bigger than the other one, below the TM_{21} patch. Due to the decision of eliminate the substrate outside the patch in the TM_{21}, the effects of the

fringing fields there are more important, and it will effect to the dimensions of both patches.

Firstly the design was taking account a 1.5 mm substrate in order to maintain the 3 mm of the first proto, but, due to the narrow separation between patches, the performance obtained wasn't the desired. So finally the decision was keep it with the same material of 3 mm for both elements.

So the finals dimensions of the prototype 2 (Figure 35) are a radius of 29.14 mm for the TM_{21} patch, without more substrate, and a radius of 37.77 mm for the other patch with a substrate of radius 52.88 mm.

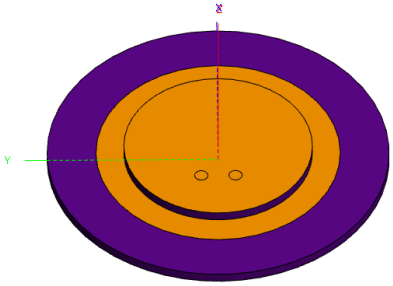

Figure 35. Proto2

In terms of feeding points (Figure 36), as is exposed before, in the case of TM_{21} (port 3 and 4) must be separated 45º and for the TM_{31} an angle of 30º. In order to keep the symmetry of the structure, the four points will be positioned with respect to the same axis. Due to that the difference between TM_{31} ports (port 1 and 2) is going to be 90º. The feedings of the TM_{21} will be positioned 13.84 mm from the middle and, in the case of the TM_{31}, 23.04 mm.

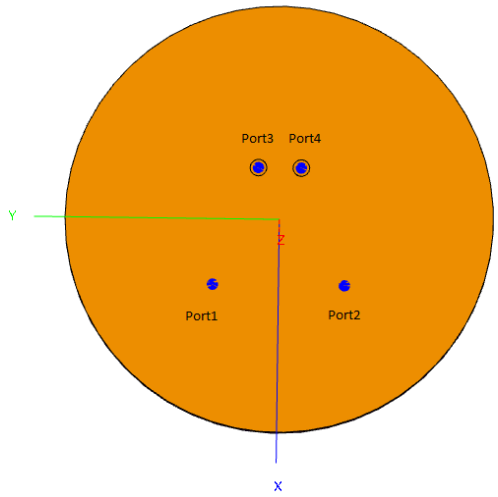

Figure 36. Proto2 Feeding Points

After the tuned the reflection coefficient for the four ports are quite good, more than -10 dB at 2.45 GHz (Figure 37). Port 1 and 2 are the feeding points of the TM_{31} circular patch antenna and port 3 and 4 are in the TM_{21} patch. As it can be seen in the case of TM_{31} is more narrowband than the other patch.

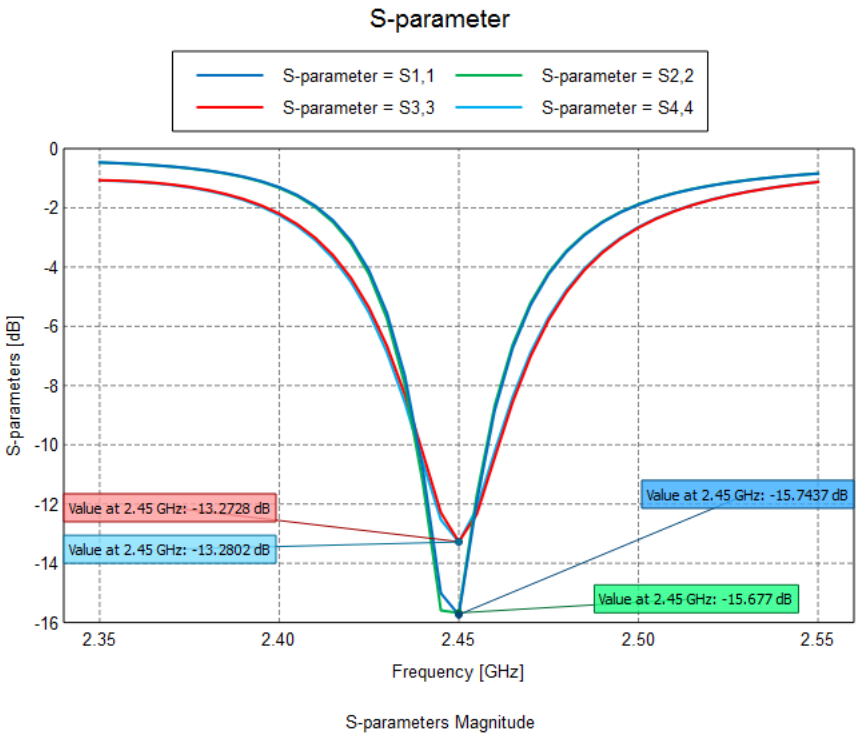

Figure 37. Proto2 S-parameters

In terms of isolation (Figure 38), is good enough for all the ports, but in the case between the ports from the patch TM_{31} and TM_{21} positioned on the same half of the structure is lowest and it can provide less efficiency.

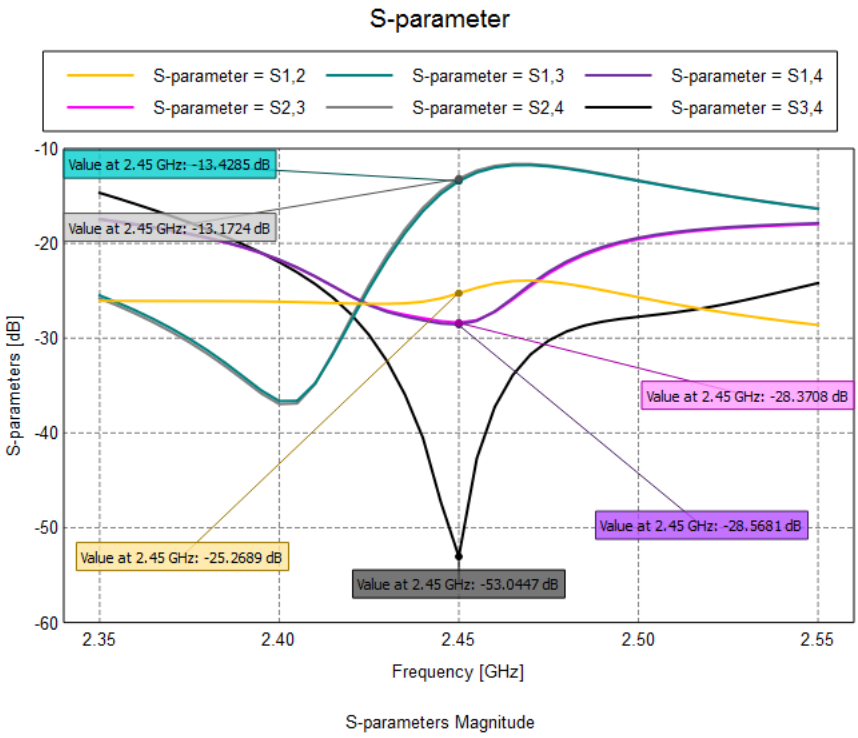

Figure 38. Proto2 Isolation

Looking at the efficiency (Figure 39), again charging the other ports with 50Ω, in the case of the circular patch TM_{21} the value simulated is around 70%, higher than the case of the TM_{31}, around 40%.

It is due to the isolation between ports in TM_{21} is much more higher, and the energy lost from one port to the other is lowest, and, also some efficiency lost is due to the tangent losses from the substrate and in the case of the TM_{31} is bigger.

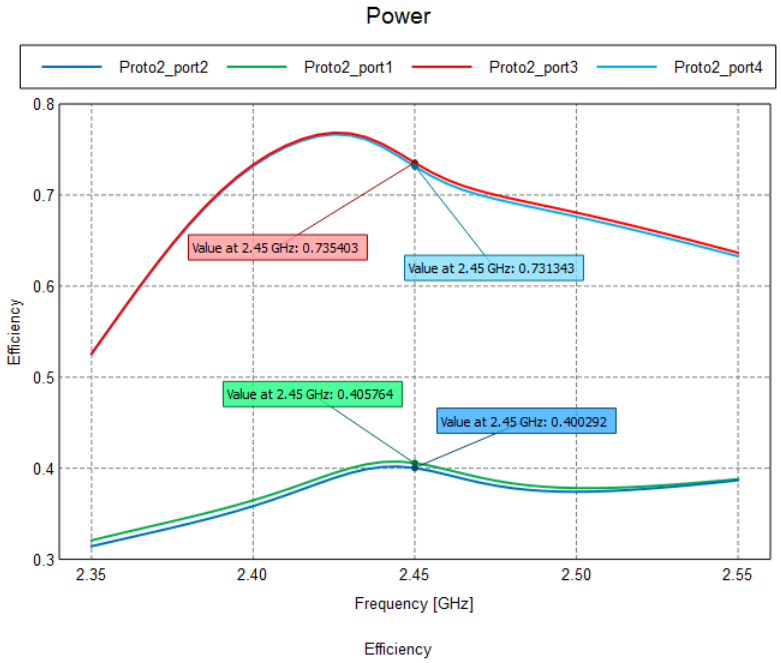

Figure 39. Proto2 Efficiency

If we pay attention to the theta component of the magnitude of far field for this second prototype, in the case of the patch TM_{31} there appears the six lobes (Figure 40), due to the currents distribution, for each one of the ports. And for the other case, there appear the expected 4 lobes (Figure 41). So with the combination of both orthogonal modes of the same patch a constant value for the magnitude in the far field is obtained.

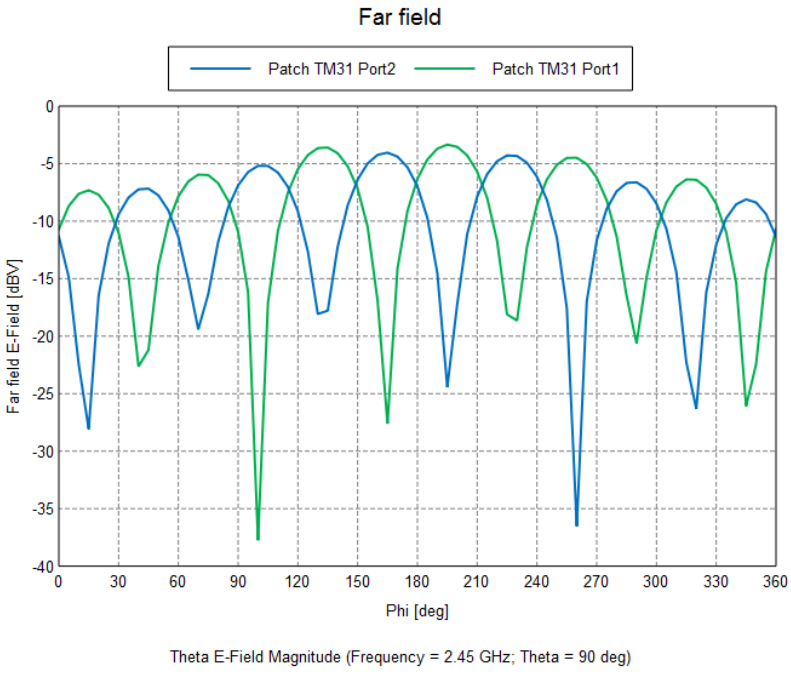

Figure 40. Proto2 TM_{31} Far Field Theta component Magnitude at 2.45GHz

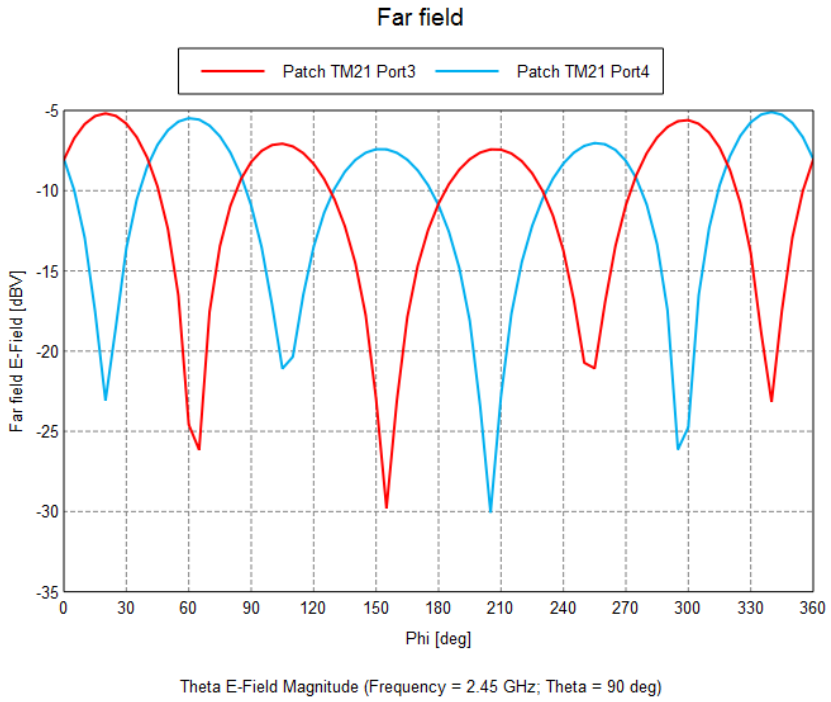

Figure 41. Proto2 TM_{21} Far Field Theta Component Magnitude at 2.45GHz

The combination of both radiation pattern from the ports of the same patch, taking account the phase difference of 90º needed between feedings, like in the case of the prototype 1, is obtained an almost constant value of magnitude for both patches (Figure 42).

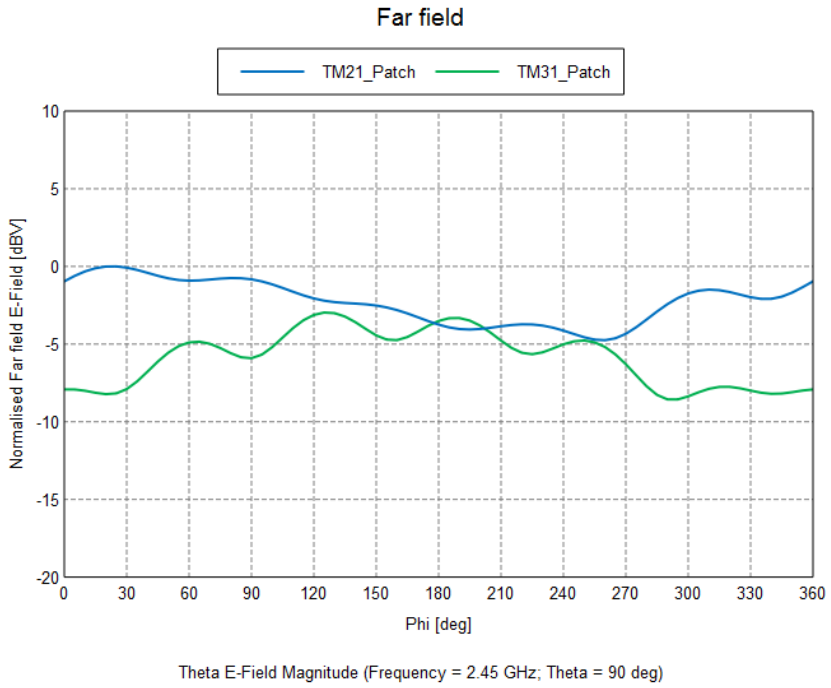

Figure 42. Proto2 far Field Magnitude Combined Theta component at 2.45 GHz

The key point in the behaviour of the concept is the far field phase, looking at the four ports performance separately there are the four degrees of freedom that can be combined in order to obtain a better functionality of the concept (Figure 43).

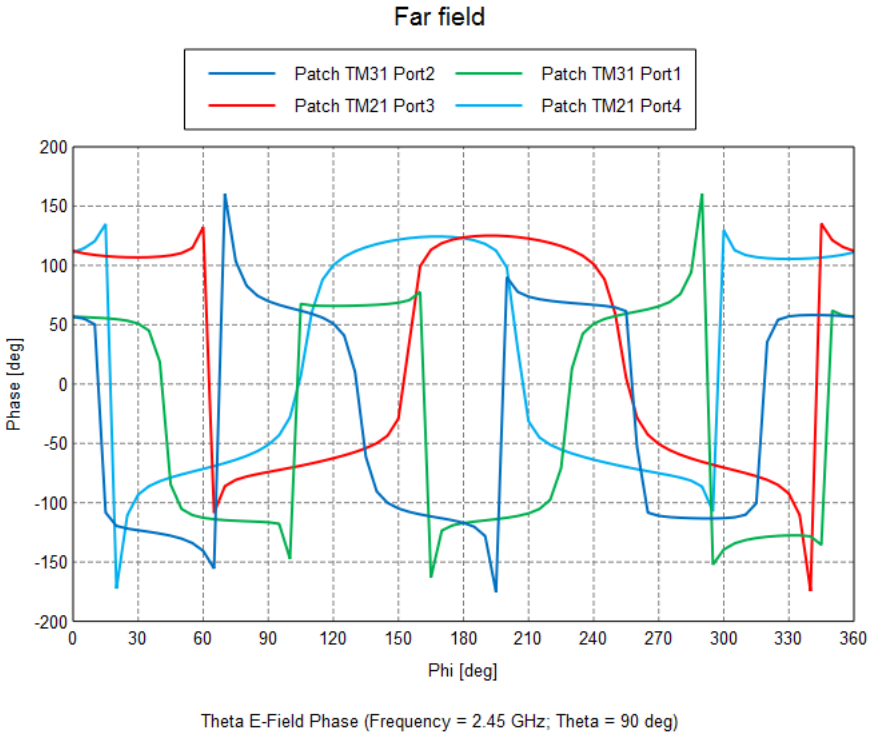

Figure 43. Proto2 Far Field Phase 4 ports Theta component at 2.45GHz

As it has seen before, in order to show in a more clearly way the behaviour, both feeding phases of ports from each patch have been simulated with a fix difference of 90º, the plot obtained from that is something similar to the performance shown in the prototype 1, where two phases are lineal dependent of the angle, are matched periodically (Figure 44). If the transmitter plays with the four phases separately, four degrees of freedom, this points where the phases are matched are less common and it eliminates this bidirectionallity shown in the prototype 1.

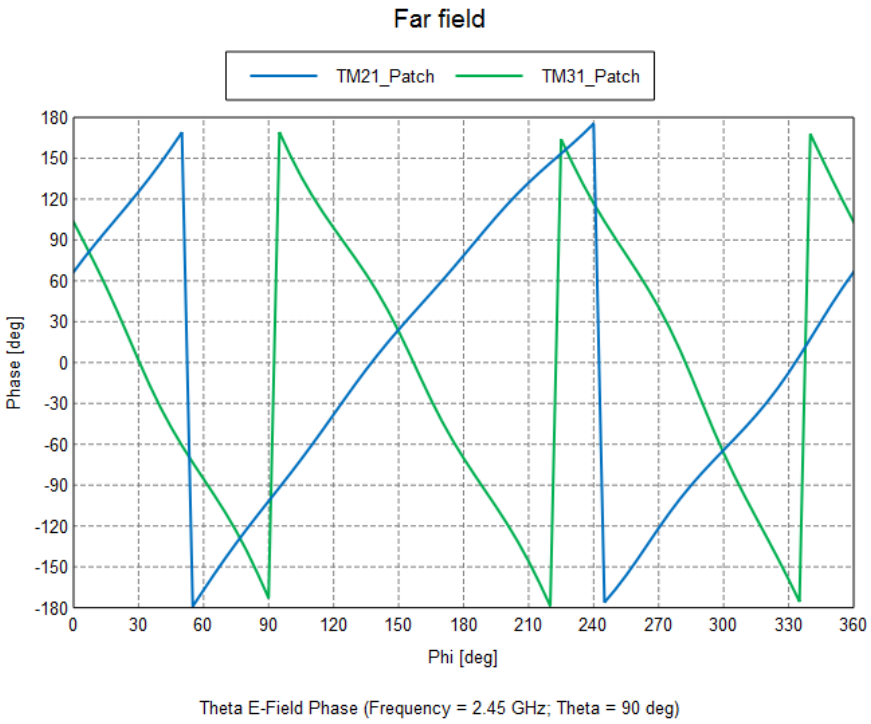

Figure 44. Proto2 Far Field Phase 2 ports

3.4. Conclusions

The conclusions that can be extracted from this third chapter are:

1. The radiation pattern analysis will be by means of the theta component because in the monopole the phi component is almost null and these criteria will be kept along all the project.
2. The first prototype, that follows the concept shown in the references [3][4], seems that works perfectly as was expected. The behaviour of the far field phases is the needed for the implementation of directional modulation that allows to substitute an array of antennas by the compact structure.
3. The prototype 1 has a patch radius is 27 mm, the substrate radius is 37.8 mm and the monopole length has a value of 3.09 cm. The patch feeding points are located in a radius of 13.23 mm, with a difference between them of 45º as is said before.
4. The second prototype is an improvement of the concept, accomplishing a similar performance but with one more degree of freedom for the directional modulation and with a more compact and robust structure.

5. The finals dimensions of the prototype 2 are a radius of 29.14 mm for the TM_{21} patch, without more substrate, and a radius of 37.77 mm for the other patch with a substrate of radius 52.88 mm.

4. EXPERIMENTAL RESULTS

This chapter pretends to validate the previous simulated results through an experimental procedure. To do so, a prototype has been built and tested for the sake of demonstrating the effectiveness of the proposal.

4.1. First Prototype

The first prototype, as is mentioned in previous chapters, consists of a copper monopole over a circular patch antenna. Table 3 shows the design specification related to the fabrication of the prototype, for instance the material used to build or the dimensions of the elements.

Specification		Value
Circular Patch Antenna	Patch radius	r_p = 27 mm
	Substrate material	TRF-45
	Substrate thickness	h = 3 mm
	Substrate radius	r_s = 37.8 mm
	Connector	SMA square flange jack receptacle
	Connector position	r_c = 13.23 mm
Monopole Antenna	Monopole length	l = 3.09 cm
	Monopole thickness	h_m = 1.3 mm
	Material	Copper
	Connector	SMA end launch jack receptacle

Table 3. Proto1 Specifications

Figure 45 shows the DXF used to build the prototype, a file with the .DXF file extension is a Drawing Exchange Format file developed by Autodesk as a type of universal format for storing CAD models. [27]

In Figure 45 we can see the shape of each part of the structure in 2D, the biggest shape is the substrate, the second is for the patch, and the others are the holes for the connectors.

The circular patch is going to be built by means of the high-speed plotter LPFK ProtoMat S62, while the monopole and the connector is going to be built manually.

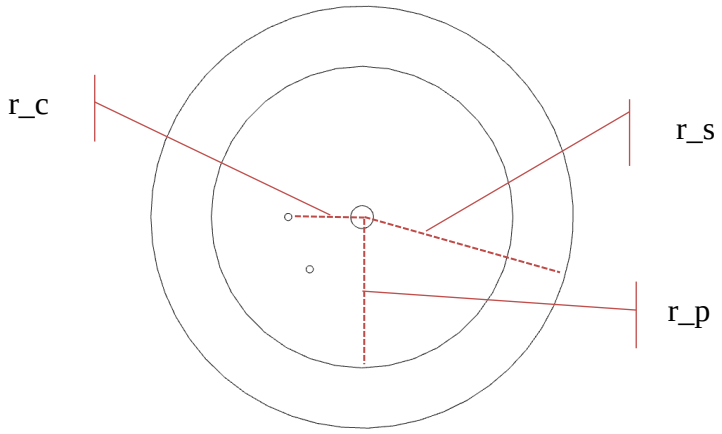

Figure 45. Proto1 DXF

4.1.1. Measurements

Once the prototype is manufactured the following steps will be the characterization and adjustment of the antennas that form the system, the antennas S-parameters and radiation patterns will be measured always in free space conditions. Notice that the ports numeration has been maintained with respect to the simulation, being ports 1 and 2 for the patch and port 3 from the monopole.

Figure 46. Proto1 S-Parameters Setup

4.1.1.1. S-Parameters

Firstly, to prove that the obtained structure will provide correct results it was studied in terms of matching. Four-port vector network analyser (VNA) was used in order to obtain s-parameter matrix. The resulting S-parameters, displayed in FEKO, are presented in the figures below.

As it can be seen in Figure 47 the point with the best matching is exactly the desired operating frequency 2.45 GHz and better than -10 dB. As was expected, the response of the patches is quite narrowband compared with the wideband response of the monopole, because of that the tuning of the monopole is much easier.

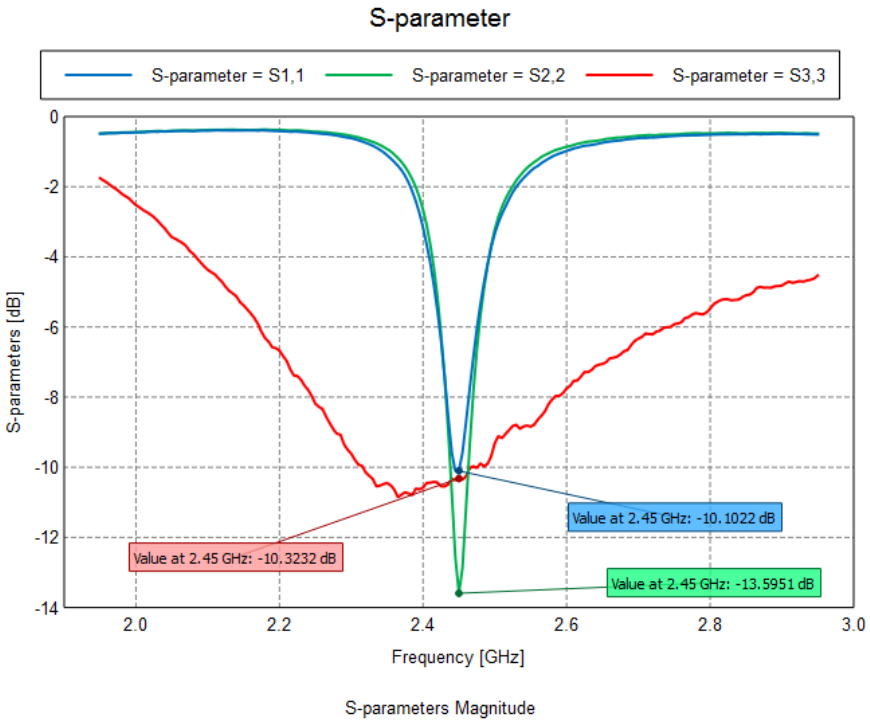

Figure 47. Proto1 S-Parameters Measured

In terms of isolation all of them are under -25 dB (Figure 48). As it can be seen the isolation between the ports of the patch is bigger than between patch and monopole, then it can be expected in a better efficiency in the patches than in the monopole. It seems that everything is working correctly in the prototype.

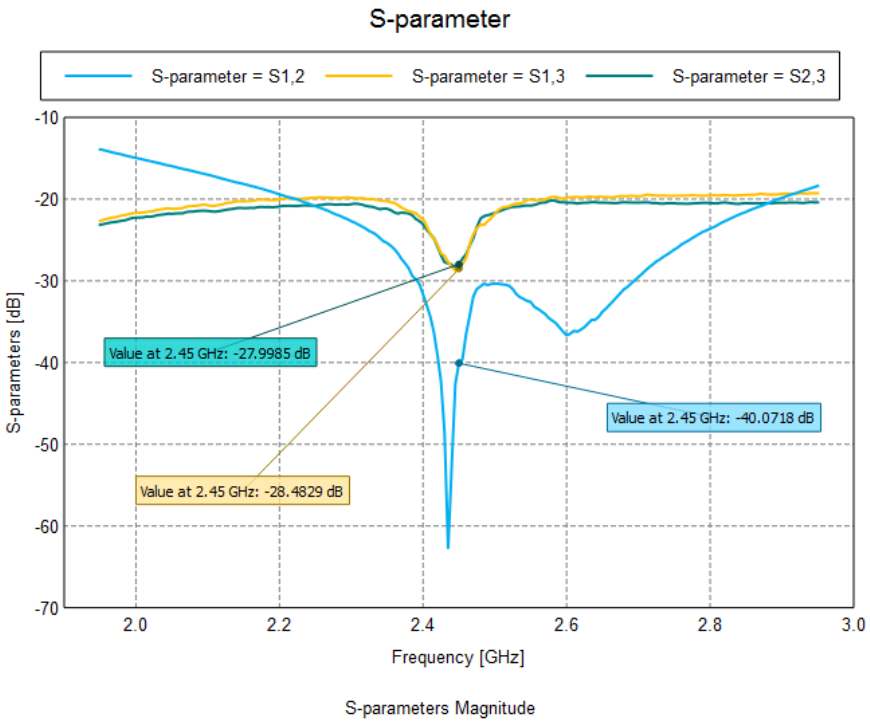

Figure 48. Proto1 Isolation Measured

4.1.1.2. Radiation Pattern

In order to prove the correct performance in terms of radiation, an anechoic chamber was used in order to obtain the radiation pattern of each antenna port separately, the antenna is fixed over a structure which rotates along its owns axis (Figure 49). The antenna rotation through its axis is equivalent to the ϕ angle and the rotation of the positioner is equivalent to θ angle.

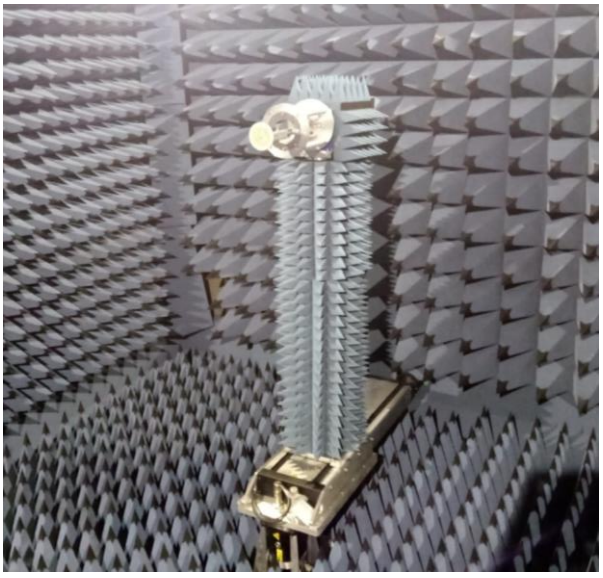

Figure 49. Proto 1 Radiation Pattern Setup

The radiation patterns are the expect ones for this kind of current distributions. The Figure 50 plots the Theta component for both ports of the circular patch, there appears the four lobes with the null on the top.

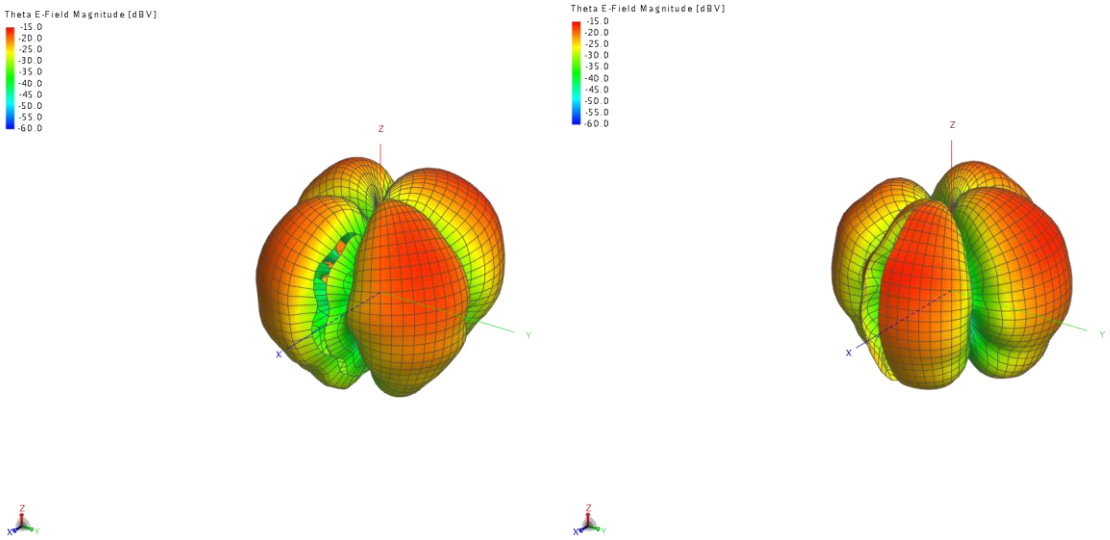

Figure 50. Proto1 Radiation Pattern Theta component Port1 and Port2 Measured at 2.45 GHz

In the case of the monopole is exactly the radiation that has seen along the simulation chapter, achieving the omnidirectional pattern (Figure 51).

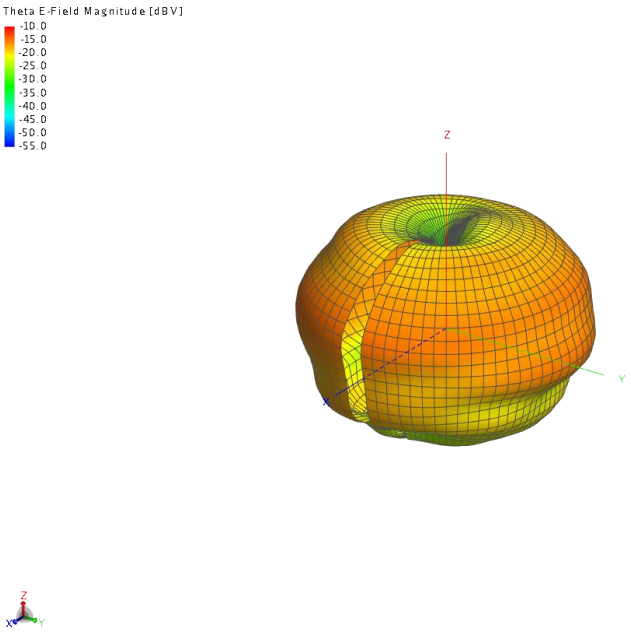

Figure 51. Proto1 Radiation Pattern Port3 Measured at 2.45 GHz

Figure 51 contains the far field theta component magnitude for each port, both cases are slightly constants, in the case of patch antenna, the combination of two ports results in that constant magnitude.

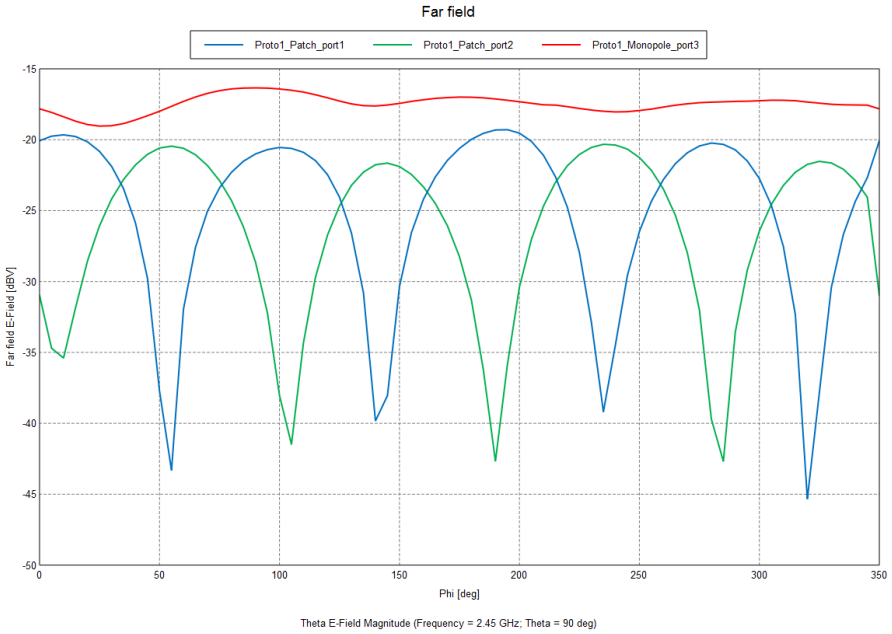

Figure 52. Proto1 Radiation Pattern Theta component Magnitude Measured Theta 90º at 2.45GHz

The far field phase behaviour is exactly the desired to be used in the application of directional modulation, the monopole has the almost constant phase and patch antenna allows playing with the phase difference between elements.

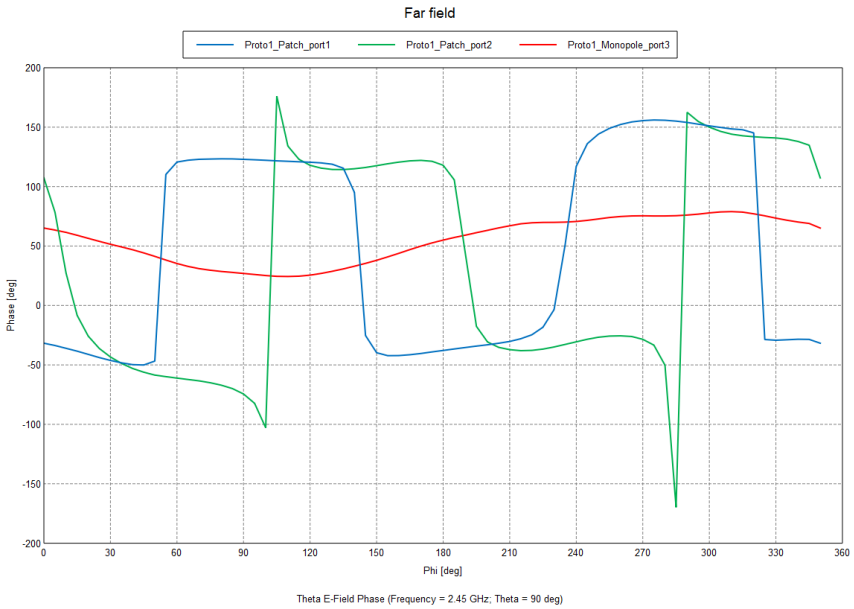

Figure 53. Proto1 Radiation Pattern Theta component Phase Measured Theta 90º at 2.45GHz

4.1.2. Simulation vs Measurements

The last step of this study is making a comparison between the measurements and the simulations results.

In terms of antenna matching, the operation frequency is exactly the same as was simulated, 2.45 GHz, and with regard to the value the measurements are lightly better than in the simulation.

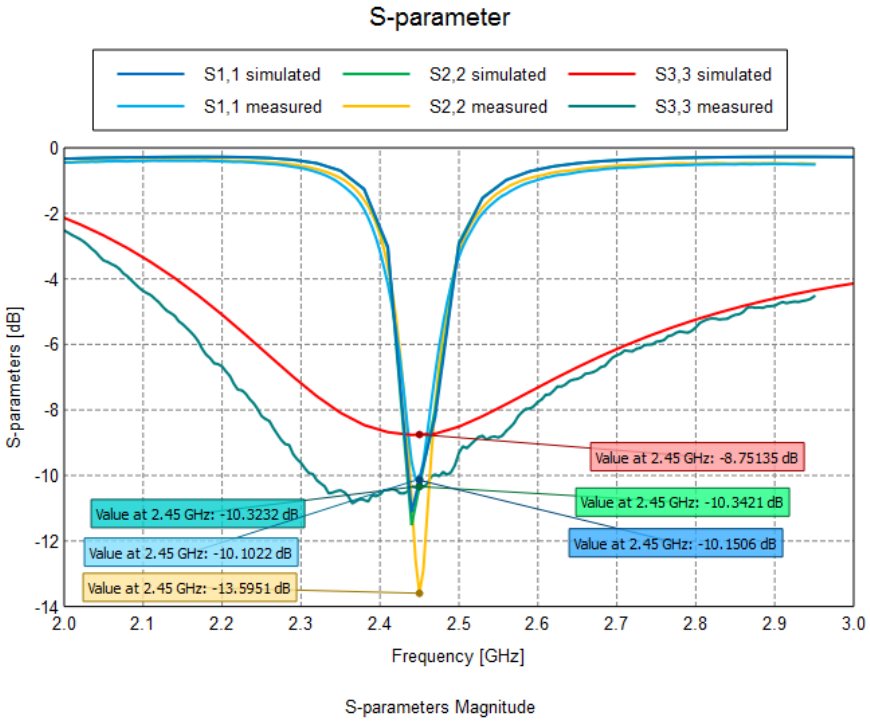

Figure 54. Proto1 S-parameters Measured vs Simulated

As in the case of matching, the isolation measurements are very similar to the value obtained in the simulation, better than -25 dB between ports.

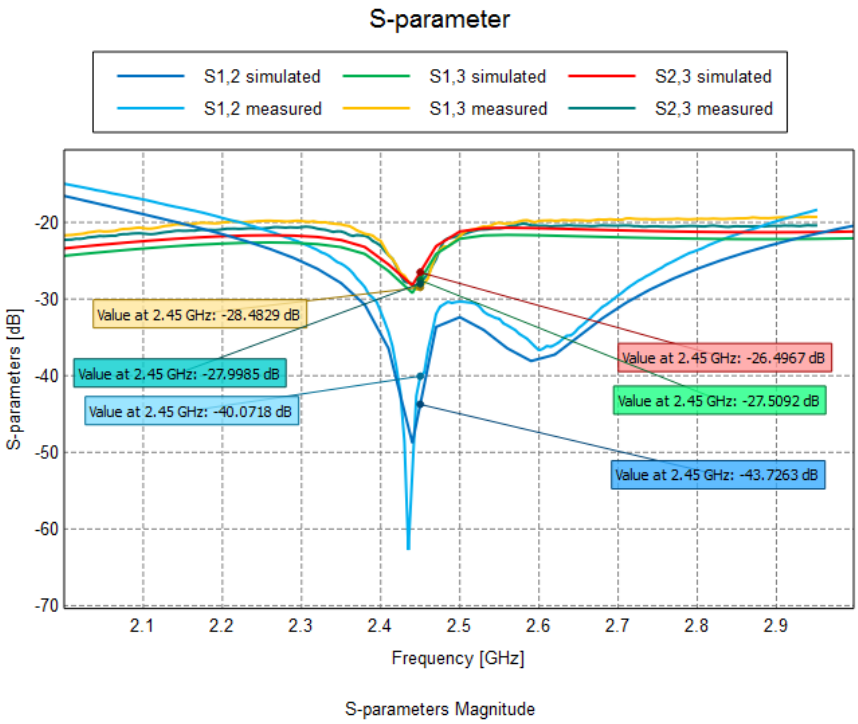

Figure 55. Proto1 Isolation Measured vs Simulated

Table 4 shows a summary of the comparison explained in Figure 54 and Figure 55.

Requirement	Measurement	Simulation
Operation frequency	2.45 GHz	2.45 GHz
Antenna matching Port1	S_{11} = -10.1 dB	S_{11} = -10.1 dB
Antenna matching Port2	S_{22} = -13.6 dB	S_{22} = -10.3 dB
Antenna matching Port3	S_{33} = -10.3 dB	S_{33} = -8.7 dB
Coupling Port1 and Port2	S_{12} = -40 dB	S_{12} = -43.7 dB
Coupling Port1 and Port3	S_{13} = -28.5 dB	S_{13} = -27.5 dB
Coupling Port2 and Port3	S_{23} = -28 dB	S_{23} = -26.5 dB

Table 4. Proto1 Requirements Measurement vs Simulation

The far field of each port of the patch antenna is combined by means of a Matlab script in order to plot the patch antenna behaviour when there is a 90º phase difference between those ports.

The Figure 56 shows the angle dependence of the phase in the circular patch antenna over the XY plane, shown during the chapter three and the almost constant phase in the monopole. And the magnitude is almost constant also in both cases (Figure 57).

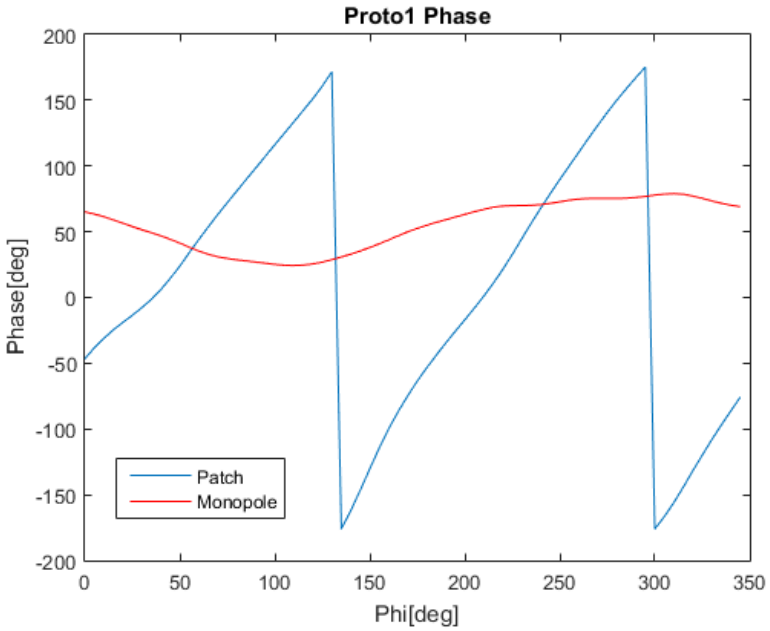

Figure 56. Proto1 Radiation Pattern Combination Phase Measured Theta 90º at 2.45GHz

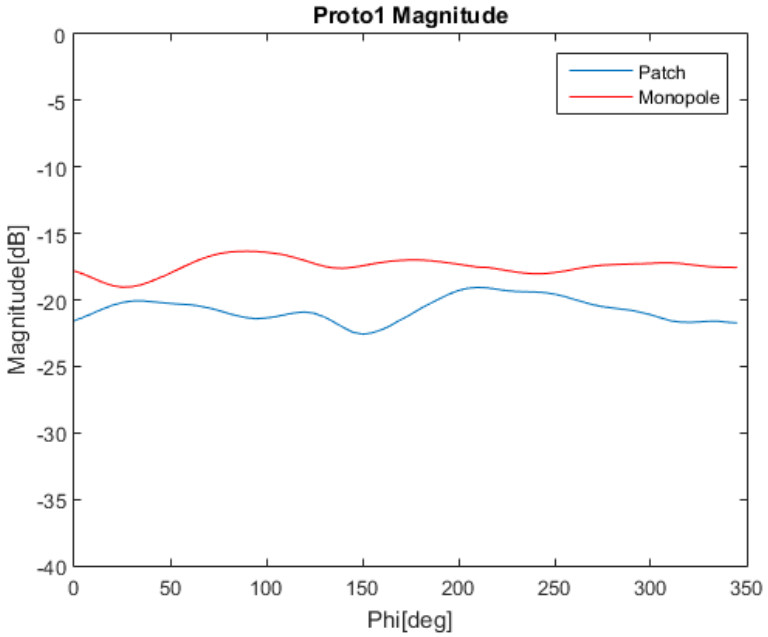

Figure 57. Proto1 Radiation Pattern Combination Magnitude Measured Theta 90º at 2.45GHz

4.2. Second Prototype

The second prototype, as is shown in the last chapter, consists of a circular patch antenna over another circular patch antenna. The Table 5 shows the design specification related to the fabrication of the prototype, for instance the material used to build or the dimensions of the elements.

Specification		Value
Circular Patch Antenna TM_{21}	Patch radius	r_p_{21} = 29.14 mm
	Substrate material	TRF-45
	Substrate thickness	h = 3 mm
	Substrate radius	r_s_{21} = 29.14 mm
	Connector	SMA square flange jack receptacle
	Connector position	r_c_{21} = 13.84 mm
Circular Patch Antenna TM_{31}	Patch radius	r_p_{31} = 37.77 mm
	Substrate material	TRF-45
	Substrate thickness	h = 3 mm
	Substrate radius	r_s_{31} = 52.88 mm
	Connector	SMA end launch jack receptacle
	Connector position	r_c_{31} = 23.04 mm

Table 5. Proto2 Specifications

In Figure 58 there are the shape of each part of the structure in 2D, the biggest shape is the substrate for the TM_{31}, the second is for the patch TM_{31}, the third one is the patch TM21, and, in that case, the substrate also, and the others are the holes for the connectors.

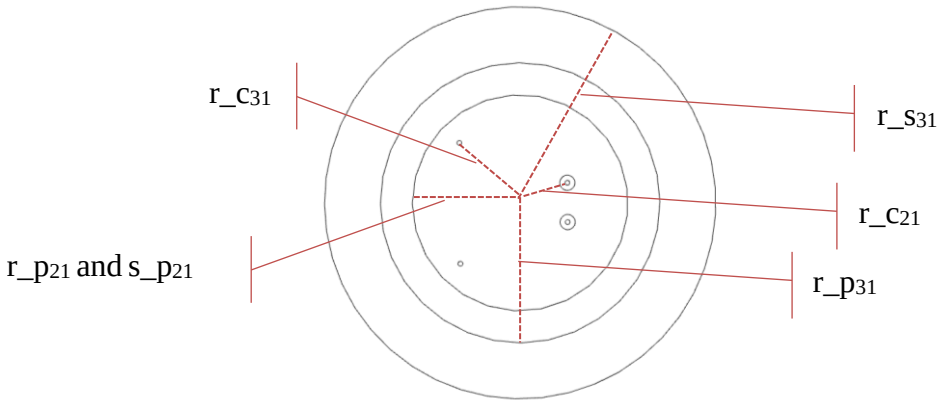

Figure 58. Proto2 DXF

4.2.1. Measurements

For this second prototype, the next step will be the characterization and adjustment of the antennas that form the system, the antennas s-parameters and radiation patterns are going to be measured in free space conditions. In that case the ports numeration is ports 3 and 4 for the patch TM_{21} and ports 1 and 2 for the other patch.

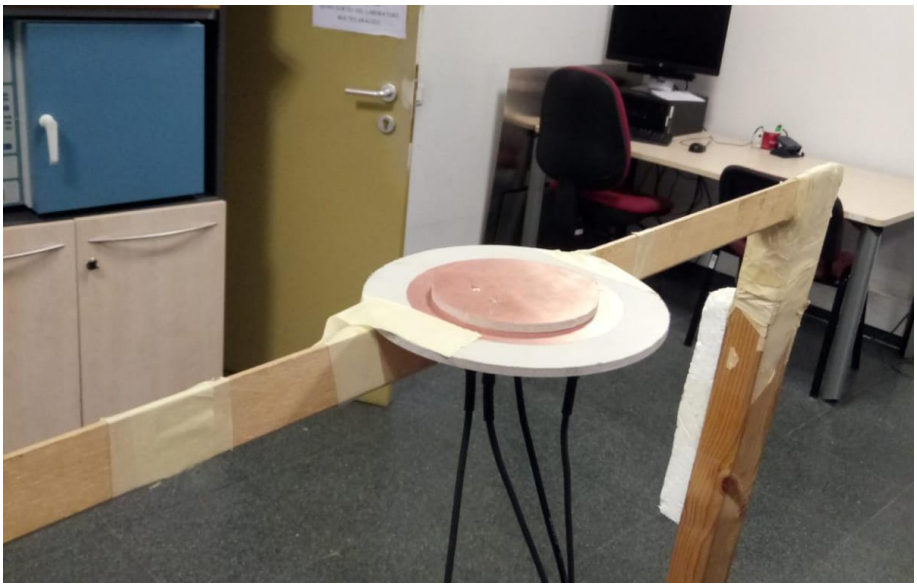

Figure 59. Proto2 S-Parameters Setup

4.2.1.1. S-Parameters

The first s-parameters measurements of this second prototype displays a great difference with the expected behaviour, the circular patch TM_{31} performance is almost the desired, but the other patch have been shifted almost 200MHz to a higher frequency (Figure 60).

This problem is due to the gap between both patches, because the air permittivity is lower than the permittivity of the substrate and, it has been explained before in the chapter two, a lower permittivity increase the operation frequency, this gap is a key point in the fabrication of the second prototype. In order to reduce the distance between patches the soldering of the feeding points from the patch below must be very accurate.

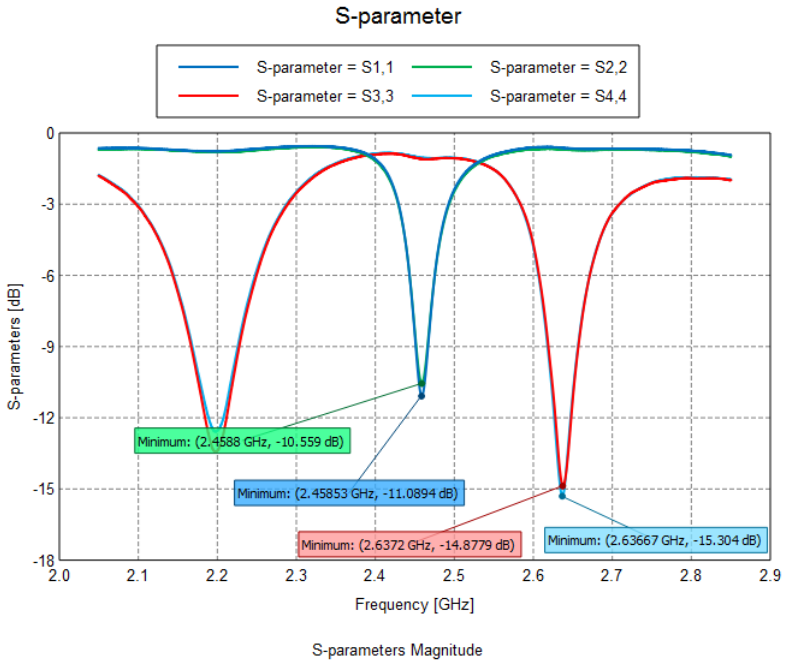

Figure 60. Proto2 S-Parameters Measured

After a tuning of the second prototype, reducing the gap between the patches by means of a better ports soldering for the TM_{31}, the response is closer to the expected in the simulation (Figure 61). There is even a slight frequency shift due to the gap and the surface roughness of the material, but much better than in the first measurement. In terms of isolation all of them are under -18 dB (Figure 62).

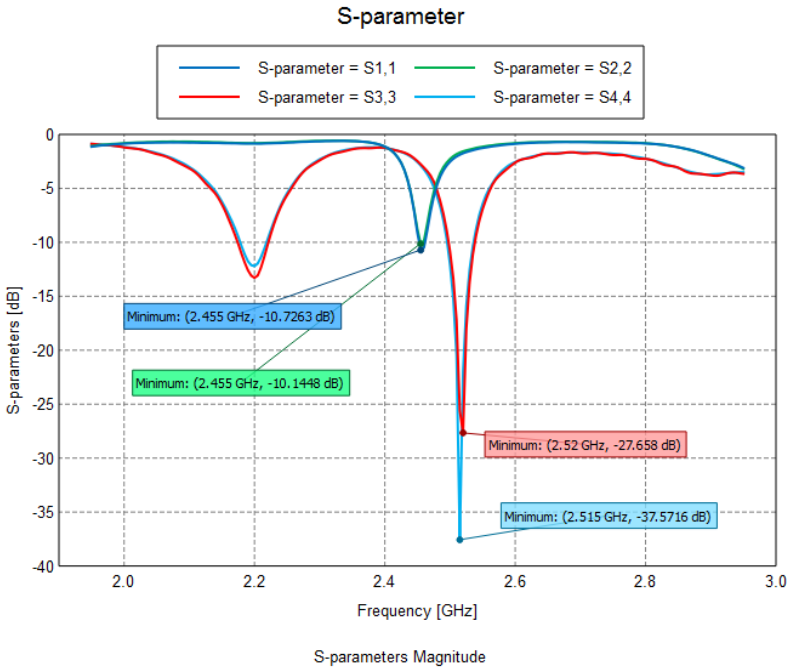

Figure 61. Proto2 S-Parameters Measured Tuned

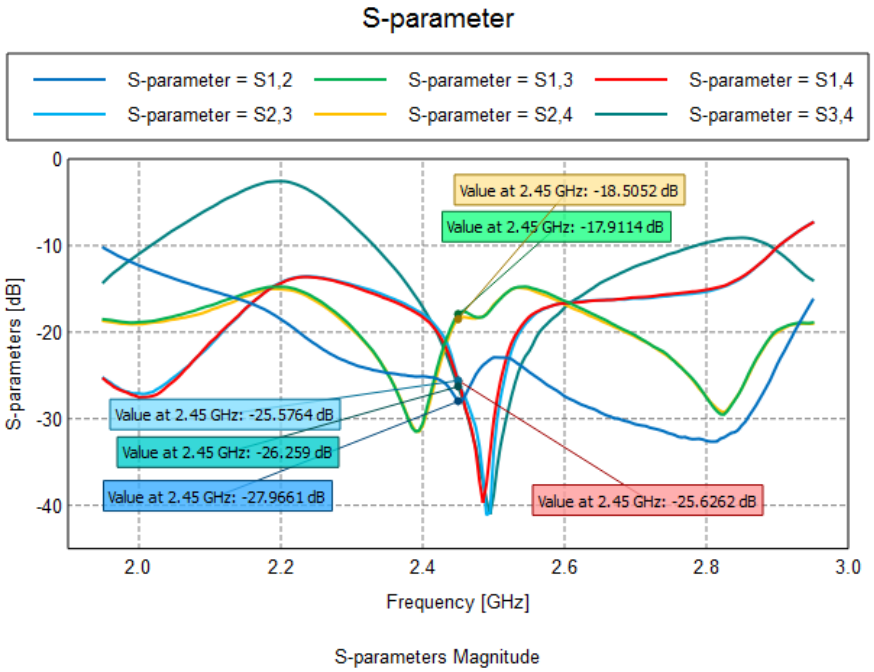

Figure 62. Proto2 Isolation Measured

4.2.1.2. Radiation Pattern

In order to prove the correct performance in terms of radiation, an anechoic chamber was used in order to obtain the radiation pattern of each antenna port separately, the antenna is fixed over a structure which rotates along its owns axis (Figure 63). The axis are the same than in the case of the prototype1.

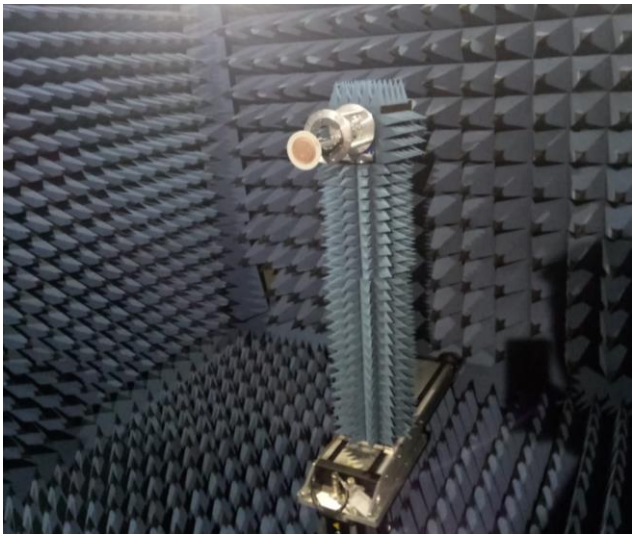

Figure 63. Proto 2 Radiation Pattern Setup

Figure 64 contains the far field theta component magnitude for the ports of the patch TM_{21}, there are the four expected lobes, and the combination of two ports results in that constant magnitude.

Figure 65 shows the same behaviour but in the case of the patch TM_{31} with the six lobes instead of the four shown in the other patch.

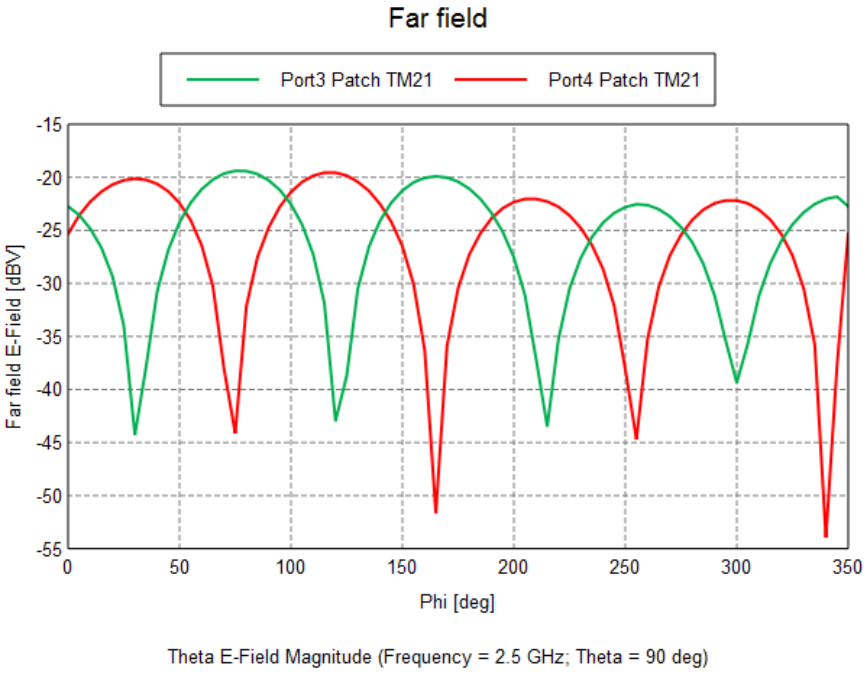

Figure 64. Proto2 Radiation Pattern Theta component Magnitude Measured Theta 90º at 2.5GHz

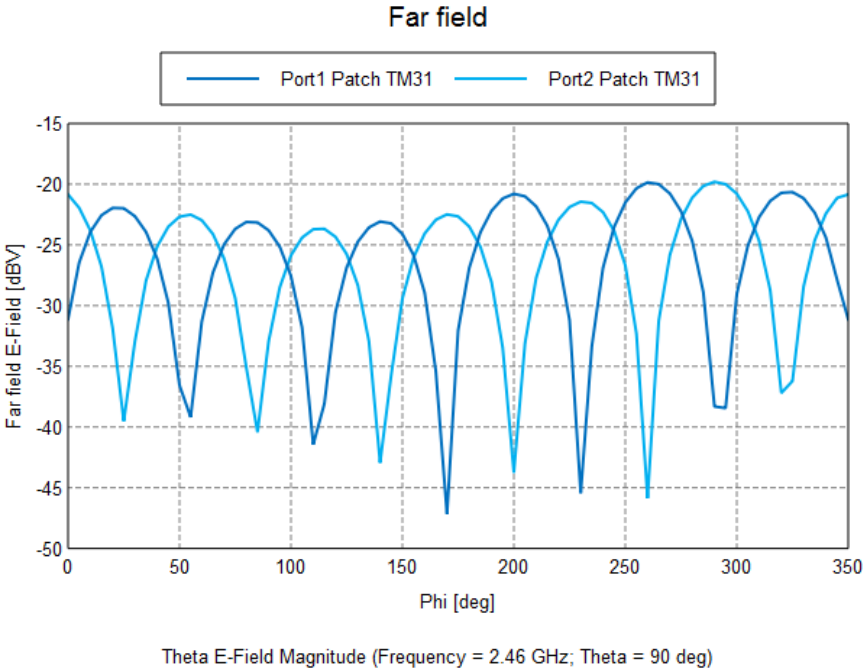

Figure 65. Proto2 Radiation Pattern Theta component Magnitude Measured Theta 90º at 2.45GHz

The far field phase of each port shown in Figure 66 will be better analyzed after the combination of the two ports of the same circular patch.

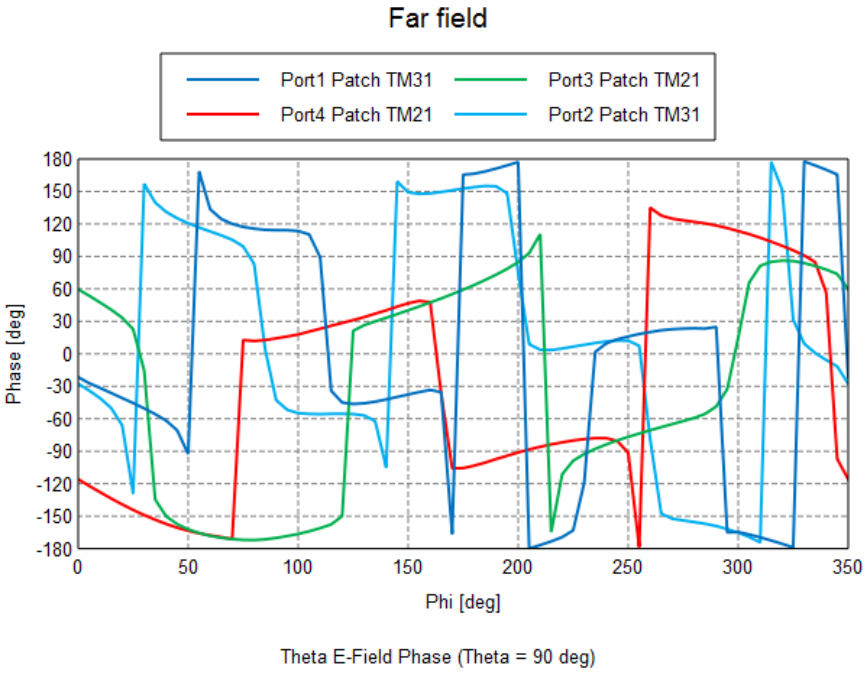

Figure 66. Proto2 Radiation Pattern Theta component Phase Measured Theta 90º

4.2.2. Simulation vs Measurements

Table 6 shows a summary of the comparison between the measurements and the results of the simulation. As was explained before, the prototype response is a little bit shifted in frequency in the TM_{21} patch due to the air gap between patches.

The antenna matching for the patch TM_{31} is much better than the simulated results, but all of them accomplish the expected requirements of -10 dB.

Requirement	Measurement	Simulation
Operation frequency	2.45 GHz for TM_{31} and 2.52 GHz for TM_{21}	2.45 GHz
Antenna matching Port1	S_{11} = -10.72 dB	S_{11} = -15.74 dB
Antenna matching Port2	S_{22} = -10.14 dB	S_{22} = -15.68 dB
Antenna matching Port3	S_{33} = -27.65 dB	S_{33} = -13.27 dB
Antenna matching Port4	S_{44} = -37.57 dB	S_{44} = -13.28 dB
Coupling Port1 and Port2	S_{12} = -27.96 dB	S_{12} = -25.27 dB
Coupling Port1 and Port3	S_{13} = -17.94 dB	S_{13} = -13.43 dB
Coupling Port1 and Port4	S_{14} = -25.62 dB	S_{14} = -28.57 dB
Coupling Port2 and Port3	S_{23} = -25.57 dB	S_{23} = -28.37 dB
Coupling Port2 and Port4	S_{24} = -18.5 dB	S_{24} = -13.17 dB
Coupling Port3 and Port4	S_{34} = -26.26 dB	S_{34} = -53.04 dB

Table 6. Proto2 Requirements Measurement vs Simulation

As it has seen before, in order to show in a more clearly way the behaviour, both feeding phases of ports from each patch have been combined with a fix difference of 90º, the plot obtained from that is something similar to the performance shown in the simulation, where two phases are lineal dependent of the angle, are matched periodically (Figure 68). If the transmitter plays with the four phases separately, four degrees of freedom, this points where the phases are matched are less common and it eliminates this bidirectionallity shown in the prototype 1.

In terms of magnitude the result of the combination is the almost constant value for both patches (Figure 67).

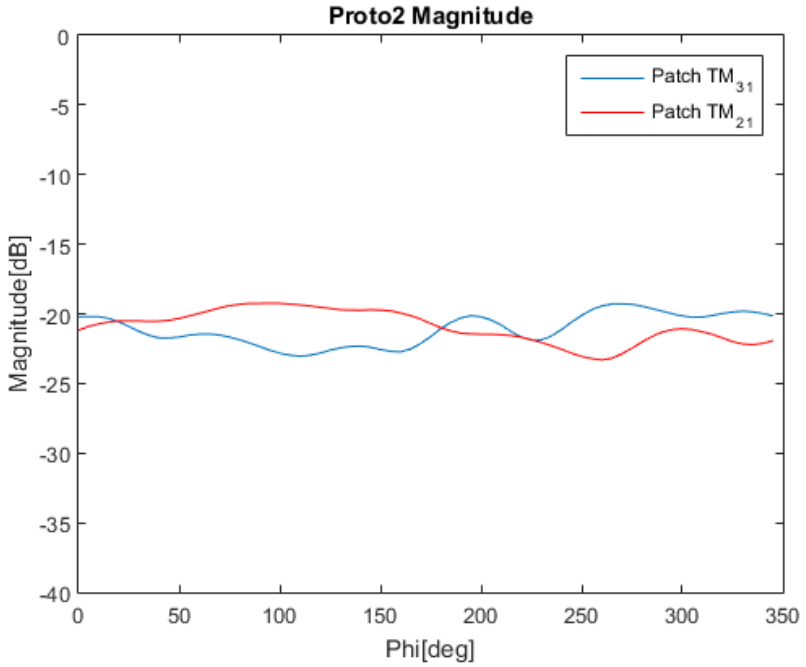

Figure 67. Proto2 Radiation Pattern Combination Magnitude Measured Theta 90º

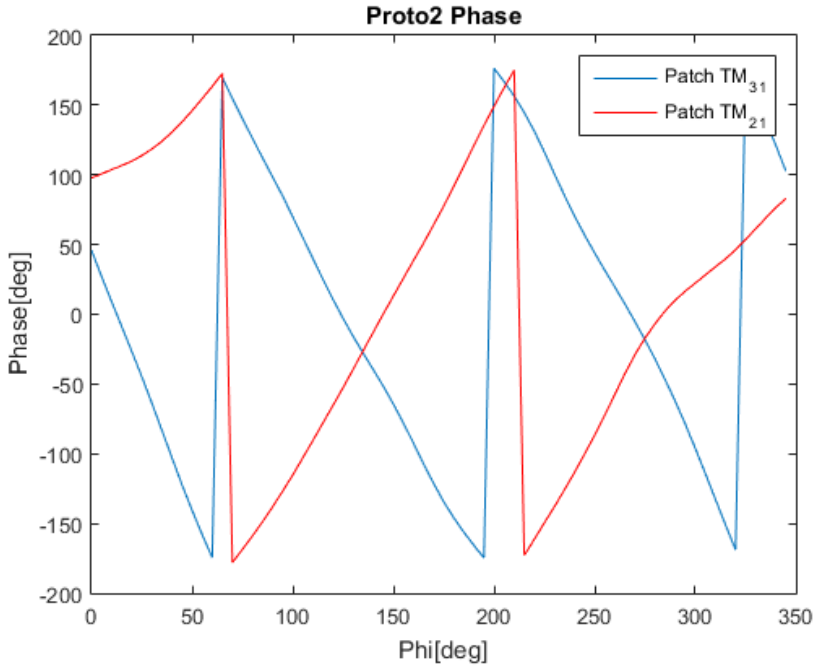

Figure 68. Proto2 Radiation Pattern Combination Phase Measured Theta 90º

4.3. Conclusions

The conclusions that can be extracted from this last chapter are:

1. The feasibility of both prototypes has been achieved by providing the needed behaviour for the implementation of directional modulation.
2. The second prototype measurements displays a difference with the expected behaviour, the patch TM_{21} have been shifted in frequency due to the air gap between patches.
3. The requirements in terms of s-parameters have been accomplished in both prototypes.
4. The antenna radiation patterns phase, after the combination of both ports from the same patch fixing the difference between them to 90º, has the expected linear dependence from the angle ϕ and a constant value for the magnitude.
5. Finally will be done a comparison between the reference [3] and the prototype 1. In terms of dimensions, using a different substrate, the thickness for the [3] is the double, the patch antenna radius is almost the same, our antenna is 1mm bigger, and, in our structure, the monopole lenght is 2 mm larger. In terms of s-paramenters their reponse is a little bit shifted in frequency between simulation and measurements. And the radiation pattern is the expected for both cases, achieveing the phase dependence from the angle.
6. The second prototype is an improvement of reference [3], eliminating the monopole and creating a more compact structure. This prototype allows to imitate the behaviour of an array of 4 patches with an antenna spacing of half-wavelength between them, so a structure of 25 or 30 cm can be substituted by our compact antenna.

5. CONCLUSIONS AND FURTHER WORK

5.1. Conclusions

The main objective of this Final Master Thesis has been achieved by the implementation of [3] by means of the building of the prototype 1 at 2.45GHz, trying to verify its suitability for directional modulation, as the efficient technique of implementing an additional security level to reliable data transfer.

Following the theoretical knowledge of the microstrip antenna and the monopole behaviour the most suitable structure was implemented. The study reveals that the resonance can be moved to lower frequencies by increasing the radius dimensions of the patch.

Theoretically found dimensions were slightly corrected with the assistance of powerful electromagnetic simulation software FEKO which allows to effectively match the theoretical calculations with a real implementation of the structure under study.

Achieved 3D model of the structure with the best performance, according to simulation, was prototyped with the milling machine. After that, was evaluated with network analyser in terms of matching and isolation, and in the anechoic chamber in terms of theta component radiated fields and phases, the structure in order to be used as part of a directional modulation system was obtained.

After the good performance of this first prototype, another structure was designed. This second prototype was built in order to achieve a more robust and compact structure and add another degree of freedom for directional modulation implementation. It was composed a circular patch working on TM_{21} mode over another circular patch working on TM_{31} mode, each one of the patches had two orthogonal modes fed by a couple of ports.

The same methodology was used for the second prototyping, but the results shown a difference in the operating frequency of the patch TM_{21} due to a fabrication issue in the gap of air between patches, despite of that, the performance of the second prototype was the expected for directional modulation.

So finally, we can conclude that an array of antennas used for directional modulation can be replaced by both compacts solutions shown along the project.

5.2. Further Work

The future work of this project consists in three different options.

The first step is to make a tuning for the prototype 2 in order to achieve the operating frequency of 2.45 GHz, it can be done making bigger the patch TM_{21} in order

to make its operating frequency higher, but due to this the TM_{31} patch response will be different because there will be more substrate over the patch with a bigger permittivity than the air. So to fight against that, the patch TM_{31} will have to be smaller.

As a second option there is the possibility of implement a miniaturization in the structure in order to make easier its integration in IoT. To achieve this miniaturization the option is to build the structure with a substrate with a different permittivity.

Taking a look to the equation (1) we can extract the following relation:

$$f_{nm} \propto \frac{1}{a_e \sqrt{\epsilon_r}}$$

So increasing the permittivity of the substrate the radius of the circular patch antenna will be smaller for the same operating frequency.

As an example of that, Figure 69 shows the response for a structure as the prototype 1 but using $\epsilon_r = 9$ instead of the TRF-45. For a similar behaviour the radius of the patch is 18.7 mm instead of the 27 cm of the built prototype.

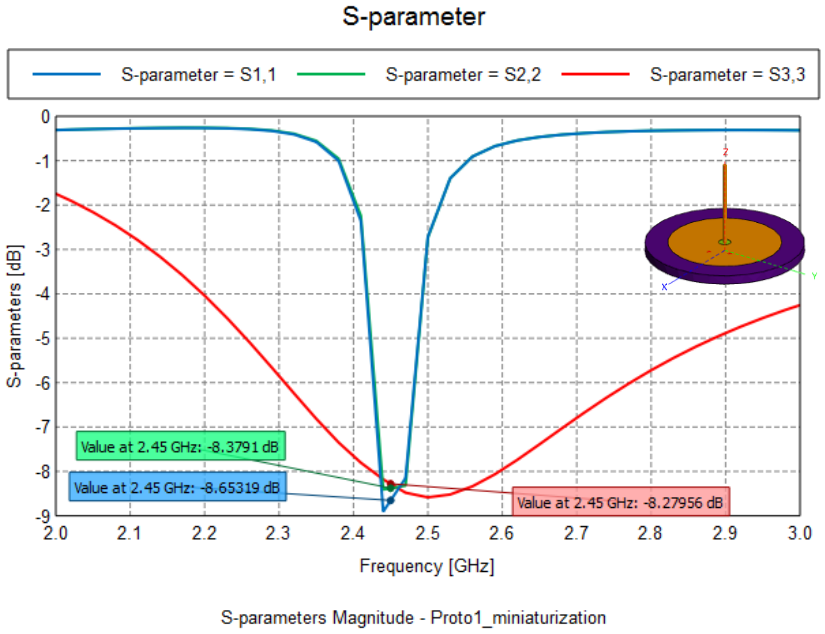

Figure 69. Proto1 Miniaturization S-Parameters

The last option is the building of another prototype introducing a third element to the prototype 2.

So this new structure will be composed of a circular patch TM21 above a circular patch TM31 and a monopole on the top of the structure. Is a kind of mix between both built prototypes, in order to achieve another degree of freedom for directional modulation.

Figure 70 shows the s-parameters of the simulation of this new prototype, it is possible to build it accomplishing the requirements of matching for all the ports.

Finally, Figure 71 plots the far field phases of both patches, with their feedings phases fixed with a difference of 90º, which have this lineal dependence from the angle and the almost constant phase of monopole.

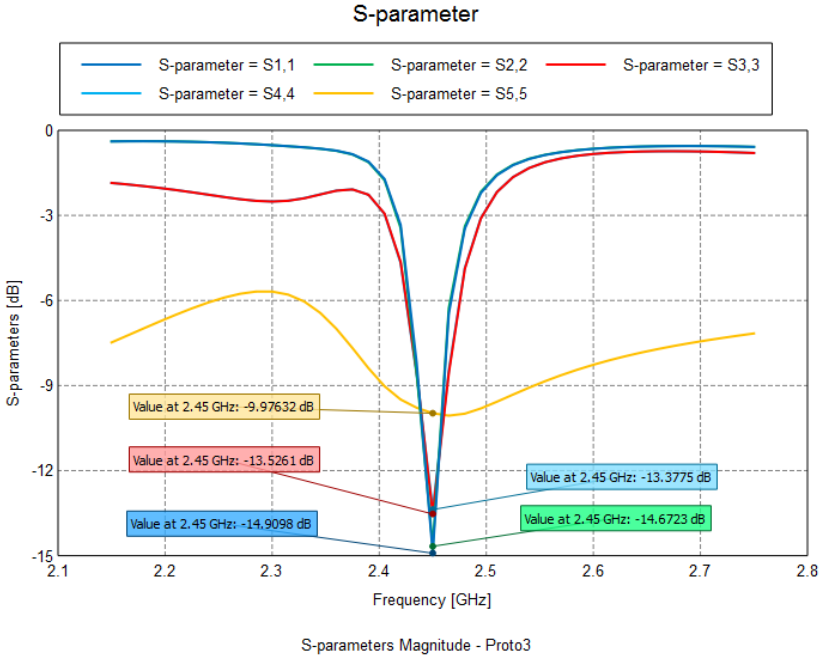

Figure 70. Proto3 S-Parameters

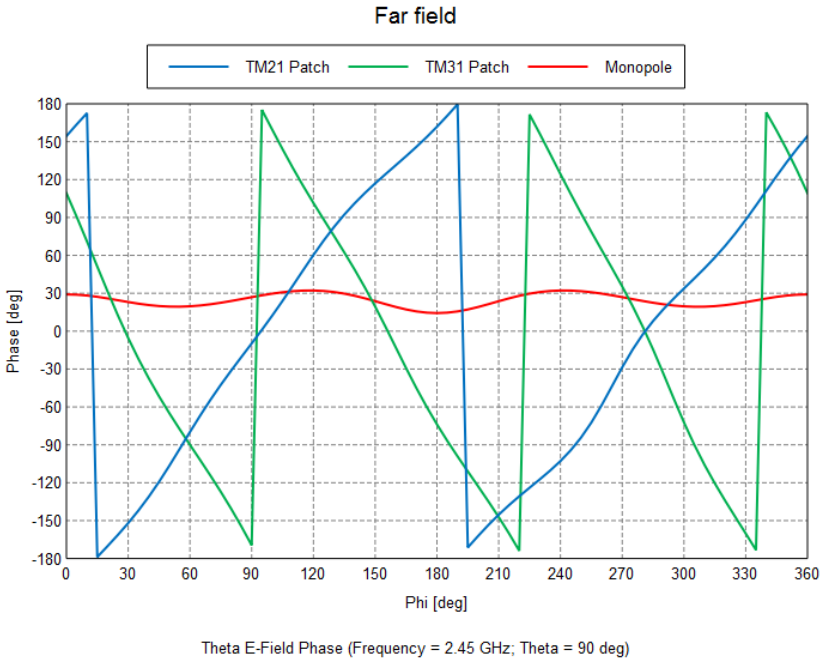

Figure 71. Proto3 Far Field Theta component Theta 90º at 2.45GHz

References

[1] "SSL (Secure Sockets Layer)". Available: https://searchsecurity.techtarget.com/definition/Secure-Sockets-Layer-SSL

[2] "IPsec (Internet Protocol Security)". Available: https://searchsecurity.techtarget.com/definition/IPsec-Internet-Protocol-Security

[3] Adam Narbudowicz, Max J Ammann and Dirk Heberling, "Switchless Reconfigurable Antenna with 360º Steering" *IEEE Antennas and Wireless Propogation Letters* vol. *15*, 2016.

[4] Narbudowicz, A., Ammann, M.J. & Heberling, D., "Directional Modulation for Compact Devices." *IEEE Antennas and Wireless Propagation Letters, vol. PP, no. 99,* 2017.

[5] W. Kummer, A. Villenueve, T. Fong, and F. Terrio, "Ultra-low sidelobes from time-modulated arrays." *IEEE Antennas Propagation, vol. 11, pp. 633–639,* 1963.

[6] B. L. Lewis and J. B. Evans, "A new technique for reducing radar response to signals entering antenna sidelobes." *IEEE Antennas Propagation, vol. 31, pp. 993-996,* 1983.

[7] S. Yang, Y. B. Gan, and P. K. Tan, "Linear antenna arrays with bidirectional phase center motion." *IEEE Antennas Propagation, vol. 51, pp. 1829-1835,* 2005.

[8] S. Yang, Y. B. Gan, and P. K. Tan, "A new technique for power-pattern synthesis in time-modulated linear arrays." *IEEE Antennas Wireless Propagation Letters, vol. 53, pp. 285-287,* 2003.

[9] S. Yang, Y. B. Gan, A. Qing, and P. K. Tan, "Design of a uniform amplitude time modulated linear array with optimized time sequences." *IEEE Antennas Propagation, vol. 53, pp. 2337-2339,* 2005.

[10] S. D. Keller, W. D. Palmer, and W. T. Joines, "Electromagnetic modeling and simulation of a directly-modulated L-band microstrip patch antenna." *In Proc. Int. Symp. on Antennas and Propagation, pp. 4489-4492,* Jun. 2007.

[11] E. Baghdady, "Directional signal modulation by means of switched spaced antennas." *IEEE Trans. Commun., vol. 38, pp. 399–403,* Apr. 1990.

[12] C. M. Elam and D. A. Leavy, "Secure communication using array transmitter." *U. S. Patent 6 275 679,* Aug. 14, 2001.

[13] A. Babakhani, D. B. Rutledge, and A. Hajimiri, "A near-field modulation technique using antenna reflector switching." *in Proc. IEEE Int. Solid State Circuits Conf, pp. 188–189,* Feb. 2008.

[14] A. Babakhani, D. B. Rutledge, and A. Hajimiri, "Transmitter architectures based on near-field direct antenna modulation." "," *IEEE J. Solid-State Circuits, vol. 43, no. 12, pp. 2674–2692,* Dec. 2008.

[15] "Getting Started Manual for FEKO 14.0," 2015. Available: https://altairuniversity.com/wp-content/uploads/2016/03/GetStarted.pdf.

[16] "Getting Started with MATLAB," 2018. Available: https://es.mathworks.com/help/matlab/getting-started-with-matlab.html.

[17] L. P. S, "A new generation of advanced circuit board plotters The new standard for in-house prototyping." Available: http://www.lpkfusa.com/datasheets/prototyping/s62.pdf.

[18] "N5242A PNA-X Microwave Network Analyzer, 26.5 GHz | Keysight (formerly Agilent's Electronic Measurement)." Available: https://www.keysight.com/en/pdx-x202277-pn-N5242A/pna-x-microwave-network-analyzer-265-ghz?cc=ES&lc=eng. .

[19] "MVG Microwave Vision Group. RF Shielded Rooms." Available: https://www.mvg-world.com/en/products/field_product_family/emc-4/rf-shielded-rooms.

[20] "Asysol Antenna systems solution." Available: http://www.asysol.com.

[21] Ding, Y. and Fusco, V., "Directional Modulation Enabled Physical-layer Wireless Security". In Trusted Communications with Physical Layer Security for 5G and Beyond. *Institution of Engineering and Technology,* 2017.

[22] Michael P. Daly and Jennifer T. Bernhard "Directional Modulation Technique for Phased Arrays", *IEEE Transactions on antennas and propagation,* vol. *57, No 9*, September 2009.

[23] Ramesh Garg, Prakash Bhartia, Inder Bahl and Apisak Ittipiboon "Microstrip Antenna Design Handbook", *Artech House Antennas and Propagation Library*, 2001.

[24] "Microstrip Patch Antennas" Available: http://www.antenna-theory.com/antennas/patches/antenna.php

[25] "The Half-Wave Dipole Antenna" Available: http://www.antenna-theory.com/antennas/halfwave.php

[26] C.A. Balanis "Antenna Theory: Analysis and Design", *3rd ed- Hoboken NJ. Wiley*, 2005.

[27] "What is a DXF File" Available: https://www.lifewire.com/dxf-file-4138558